REPUBLIC OF TURKEY
BİNGÖL UNIVERSITY
INSTITUTE OF SCIENCE

MONITORING OF CORROSION RATE USING MOLECULAR ABSORPTION SPECTROSCOPY IN GAS TREATMENT PLANT

MASTER'S THESIS

HOGR OMAR PIRDAWOOD

CHEMISTRY

THESIS ADVISOR
Prof. Dr. İBRAHİM Y. ERDOĞAN

BİNGÖL-2018

REPUBLIC OF TURKEY
BİNGÖL UNIVERSITY
INSTITUTE OF SCIENCE

MONITORING OF CORROSION RATE USING MOLECULAR ABSORPTION SPECTROSCOPY IN GAS TREATMENT PLANT

MASTER'S THESIS

Hogr Omar PIRDAWOOD

Department : CHEMISTRY

This dissertation was accepted by the following committee on 04.01.2018 with the vote unity.

Prof. Dr.	**Assoc. Prof. Dr.**	**Prof. Dr.**
Ramazan SOLMAZ	**Mehmet KAHRAMAN**	**İbrahim Y. ERDOĞAN**
Head of examining committee	**Member of examining committee**	**Member of examining committee**

I confirm the result above

Prof. Dr. İbrahim Y. ERDOĞAN

Director of the institute

PREFACE

First and foremost, praises and thanks to the God, the Almighty, for His showers of blessings throughout my research work to complete the research successfully.

I have to express my deep and sincere gratitude to my academic supervisor Prof. Dr. İbrahim Y. ERDOĞAN for providing me with the opportunity to complete my master thesis at the Bingöl University.

I also have thank for my manager and teacher, Prof. Dr. Nicola MAGARELLI who has not hesitated in helping me during my thesis work, he has been actively interested in my work and has always been available to advise me. I am very grateful for his patience, motivation, enthusiasm.

I am extremely grateful to my parents for their love, prayers, caring and sacrifices for educating and preparing me for my future.

Finally, my thanks go to all the people who have supported me to complete the research work directly or indirectly.

Hogr Omar PIRDAWOOD

Bingöl 2018

CONTENTS

LIST OF SYMBOLS AND ABBREVIATIONS

A=Abs	: Absorbance
A	: Atomic weight
B	: Optical path length of sample cell
C	: Concentration
CPS	: Central process station
CR	: Corrosion rate
D	: Density of metallic
E	: Electrical potential
E^0cell	: Cell potential under nonstandard conditions
Ecell	: Cell potential
E_{eq}	: Equilibrium potential
F	: Faraday's constant
f	: Fugacity
Ft	: Feet
g	: Gram
GTP	: Gas treatment plant
H	: Activation overpotential
I	:Transmitted Intensity
I_0	: Intensity of the ıncident light at a given wavelength.
J	: Total current density
j_0	: Current density
Ke	: Electro kinetic constant
K_W	: Water dissociation constant
L	: Liter
LPR	: Linear polarization resistance
M	: Molarity
MDEA	: Methylediethanolamine

mL	: Milliliter
MMSQF/D	: Million standard cubic feet per day
mpy	: Mils per year
N	: Number of electron lost
nm	: Nanometer
P	: Density of material
ppm	: Part per million
Q	: Reaction quotient
R	: Gas constant
s	: Seconds
t	: Time
T	: Temperature
UV	: Ultraviolet
V	: Volume
V_{gas}	: Gas velocity
W	: Mass loss in time T/kg
Z	: Number of electrons in the reaction equation for the anodic reaction
α_a	: Anodic charge transfer coefficient
α_c	: Cathodic charge transfer coefficient
Λ	: Wavelength
Mg	: Microgram
μm	: Micrometer
ϵ	: Extinction coefficient or absorptivity

LIST OF FIGURES

LIST OF TABLES

GAZ ARITMA TESİSİNDE MOLEKÜLER ABSORPSİYON SPEKTROSKOPİSİNİ KULLANARAK KOROZYON HIZININ İZLENMESİ

ÖZET

Bazı petrol gazı arıtma tesislerinde korozyon reaksiyonlarının yan ürünleri olarak ortaya çıkan iyonik demir formları, temiz gaz üretmek için yüksek asitli gazların emilmesi üzerine korozyon işleminin nasıl bir rol oynadığını anlamak için önemli bir yoldur. Korozyon, üretim eksikliği, programlanmayan ana ekipmanın çalışmasının durması ve yatırım kaybı nedeniyle çözülmesi gereken önemli bir problemdir. Irak'ta Erbil şehrinde bulunan KAR grubu da bu problemin varlığında Gaz Arıtma Kompleksinde faaliyet gösteriyor. Alan düzeyinde değerlendirme tasarımının deneysel niteliği ile burada sunulan tezde, Irak'ta KAR Grup Şirketinde Khurmala Petrol ve Gaz Sahasında bulunan Gaz Arıtma Tesisinde (GTP) moleküler absorpsiyon spektroskopisini kullanarak korozyon hızının izlemesi ve takip edilmesi hedeflenmiştir. Bu çalışmanın amacı, sıvı fazlarda çözünmüş olan demirin konsantrasyonunu ölçmek ve bu tür bir korozyondan kaynaklanan bozulmanın kontrol altına alınmasına yardımcı olmak için hidrojen sülfür (H_2S) ve karbon dioksit (CO_2) tarafından saldırıya uğramış metalurjik ortamda meydana gelen korozyon hızıyla bunu ilişkilendirmektir. Metodoloji dört kısma ayrılır: a) kalibrasyon içeren zengin metildietanolamin (MDEA) çözücüsündeki demir içeriğinin tayini için standart analitik yöntem geliştirilmesi, b) amin akışlarındaki demir konsantrasyonu ile korozyon hızı arasındaki ilişkiyi geliştirmek amacıyla yeterli veri almak için örnekleme programının uygulanması, c) Demir içeriği ve korozyon hızı arasındaki matematiksel ilişkiyi geliştirilmesi, d) kalite kontrolünün rutin bir analizi olarak demir içeriğinin rutin analizinin yapılması ve korozyon hızının tahmin edilmesi. Moleküler absorpsiyon spektroskopisine dayanan demir tayini, %97,05 doğruluk, %99,92 kesinlik, %0,08 standart sapma ve %3'ten az analitik hata ile güvenilir ve yüksek tekrarlanabilirliğe sahip bir yöntemdir. GTP'deki genel korozyon hızı, 80 MMSCFD'de ve 0,41 mol H_2S/mol MDEA yüklemesi durumunda 15,35 mpy'dir. Burada ortalama 2 aylık korozyon hızı uluslararası korozyon hızı standartlarıyla karşılaştırıldığında bu sistem, kontrol koşulları altında (sınır seviyesi 3 ile 4 arasında) yüksek korozyon hızlı sistem olarak sınıflandırılabilir. Korozyon hızını azaltmak için bazı işlemlerin yapılması gerekir. GTP'de tahrip edici testler yapılmadan rutin korozyon hızını belirlemek için bu prosedürün sürdürülmesi önerilir.

Anahtar Kelimeler: Korozyon hızı, demir içeriği, moleküler absorpsiyon spektroskopisi.

MONITORING OF CORROSION RATE USING MOLECULAR ABSORPTION SPECTROSCOPY IN GAS TREATMENT PLANT

ABSTRACT

Ionic iron forms as byproducts of corrosion reactions in some petroleum gas treatment plant is an important way to understand how corrosion process acts over absorption of highly acid gases to produce clean gas. Corrosion is an important problem to solve due to lack of production, no programmed main equipment shutdown and loss of investment. In KAR group, Erbil, Iraq is operating Gas Treatment Complex with the presence of this problem. In the present thesis with experimental nature of field level evaluation design have the object to monitor and follow up corrosion rate using molecular absorption spectroscopy occurring in the Gas Treatment Plant (GTP) in Khurmala Oil and Gas Field, KAR Group Company, Iraq. Purpose of this study was to measure the concentration of iron dissolved on liquids phases and relates this with the corrosion rate occurring in metallurgical being attacked by hydrogen sulfide (H_2S) and carbon dioxide (CO_2) in order to help to control deterioration produced by this kind of corrosion. The methodology have four parts: a) developing standard analytical method for determination of iron content in rich methylediethanolamine (MDEA) solvent including calibration, b) implementation of sampling schedule for taking enough data for developing relationship between iron concentration in amine streams and its corrosion rate, c) develop mathematical relationship between iron content and corrosion rate, d) establish routine analysis of iron content and prediction of corrosion rate as a routine analysis of quality control. Iron determination based on molecular absorption spectroscopy is a reliable and high reproducible method with accuracy of 97.05% and precision of 99.92% with a standard deviation of 0.08% and analytical error less than 3%. Overall corrosion rate in GTP is of 15.35 mpy at 80 MMSCFD and 0.41 mol H_2S/mol MDEA loading compared this average 2 months corrosion rate with international corrosion rate standards this system can be classified as high corrosion rate system but on control conditions (between borderline level 3 to 4). Some actions need to be applied to reduce corrosion rate. It is recommended to maintain this procedure to estimate routine corrosion rate in absence of no destructive tests in GTP.

Keywords: Corrosion rate, iron content, molecular absorption spectroscopy.

1. INTRODUCTION

Khurmala oil and gas project is located in Southwest Erbil-Kurdish region 15 km from Erbil city. The KAR Group, a Kurdish region based oil services company, operates the oil field named Khurmala and it has 60 wells distributed around the wells zone named: North, Middle and South wells stations. Each group of wells send oil and gas to the Central Process Station (CPS), where CPS complex is responsible for separating impurities coming with oil and gas (sludge and no desirable condensates) with production of heavy acid gases (large content of hydrogen sulfide – H_2S and carbon dioxide CO_2) and desalted crude oil for refining. Like this next block diagram shows.

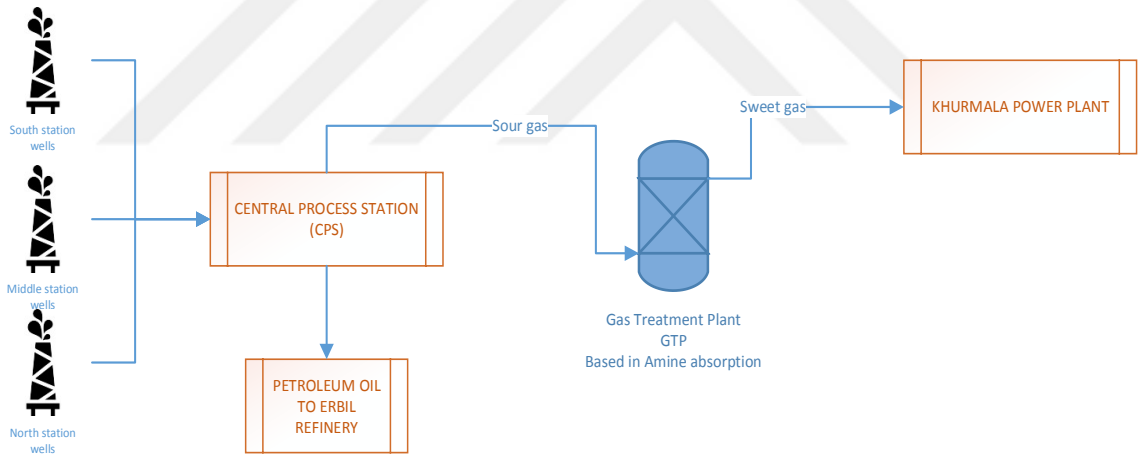

Figure 1.1. Block diagram configuration of Khurmala Oil and Gas Project

Once crude oil is cleaned, CPS by proper pump station sends crude oil to Erbil Refinery through 40 km pipeline. From the other side; heavy acid gas in large amount (250 MMSQF/D) is available out from this process, typical composition of this acid gas named *Sour Gas* because contents high level of H_2S and CO_2 is shown in (Table 1.1).

Table 1.1. Typical sour gas composition feeding GTP

Composition	Mole Percentage
Methane	76%
Ethane	9.5%
Propane	3.4%
Iso-Butane	0.3%
N-Butane	1.2%
Iso-pentane	0.5%
N-Pentane	0.4%
CO_2	5%
H_2S	3.5%
N_2	0.2%

In energy business, and Kurdish region is due to lack of electricity, KAR group built a world class Power Plant that is fed by a special *Sweet and Dried Gas* (natural gas with low concentration of acid gases and water content for energy production), For this purpose, the typical quality of sweet and dried gas needed by this power plant is shown in (Table 1.2)

Table 1.2. Typical sweet gas composition feeding GTP

Composition	Mole Percentage
Methane	82%
Ethane	9.5%
Propane	3.4%
Iso-Butane	0.3%
N-Butane	1.2%
Iso-pentane	0.5%
N-Pentane	0.4%
CO_2	3%
H_2S	0.02%
N_2	0.2%
Water	0.0094%

Consequence of this, KAR group decided to build an intermediate complex *named Gas Treatment Plant (GTP)* to treat sour gas produced by the wells into sweet/dried gas according to Khurmala Power Plant specifications and quality mentioned in (Table 1.2). Removing acid loading means, CO_2 and H_2S to very low levels to feed Khurmala Power Plant. From mole % of contaminants to ppm.

According to this, GTP unit have to take special care about corrosion all over process and, specifically over main equipment susceptible for corrosion caused by acid gases. In this way, the laboratory analysis has showed that the Khurmala natural sour gas, in normal conditions, has huge quantities of H_2S about (3.5%) and CO_2 about (5%) therefor it cause two major problems representing a significant threat to an amine gas treating plant are corrosion and instability of operation, resulting in unscheduled upsets an outages.

In other hands, sweetening process taken in Khurmala GTP is shown, sour gas is passing through absorber to produce sweet gas using special amine (mono–diethanolamine–MDEA) to catch acid loading, this amine with high level of acid gas dissolved in it (rich amine) is regenerated to be used again in a close circuit process, as can be seen, tops of absorber, regenerator tower, flash drum and condensers are under extremely corrosion process, it is important to mention GTP is mainly carbon steel constructed so, corrosion rate will be expected to be high and must be controlled to avoid lack of production due to shutdowns by this cause.

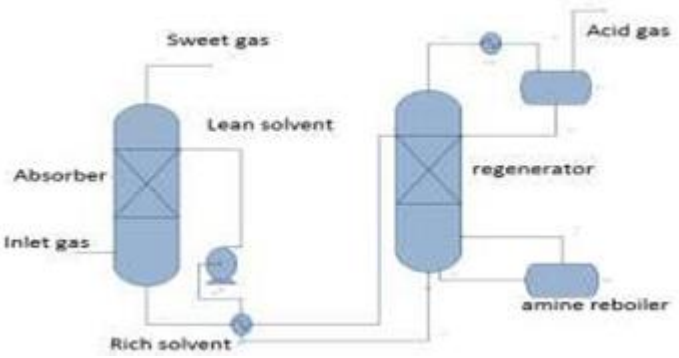

Figure 1.2. Schematic of simplified gas sweetening plant (GTP)

This GTP have the purpose to catch at least 99.5% minimum of H_2S and 30% of CO_2, that's means H_2S enter to GTP around 3.5% mole and its reduced onto sweet/dried gas to maximum 194 ppm. In this order of ideas, natural gas has a significant role in the recent world development especially for Iraq/Kurdish region who is interested to use its natural resources to get energy independence. However, natural gas usually contents acid gases for example, H_2S and CO_2 that it needs to be removed from natural gas to meet the gas pipelines specifications (Ribwar et al. 2015) as mentioned, Amine solutions are used for the removal of hydrogen sulfide (H_2S) and/or carbon dioxide (CO_2) gases before sending to power plant to making electricity, in order to create a low corrosion rate environment for the economical transportation of oil and gas to refineries and utilities. In details, Khurmala GTP alkanolamine solution (MDEA) is used to remove either H_2S or CO_2, The sour gas enters the absorber at the bottom and makes its way to the top through 21 trays. A solvent, which enters the absorber at the top, is used to remove H_2S and CO_2 from the gas mix. The most commonly used chemical solvent for hydrogen sulfide removal is MDEA. Using of methyldiethanolamine can give us better hydrogen sulfide absorption than carbon dioxide absorption. The methyldiethanolamine as used in Gas Treatment Plant, utilizes selectivity of the chemical for H_2S in Preference to CO_2 in no equilibrium situation. The reaction of H_2S with methyldiethanolamine very fast by proton transfer as is the case with other commonly used amines.

$$H_2S + R_2NCH_3 \leftrightarrow R_2NCH_4^+ + HS^- \quad (1.1)$$

CO_2 firstly reacts with water to form bicarbonate. It is the formation of the bicarbonate which is generally the slow reaction which limits the CO_2 reaction to less than equilibrium values at short contact times.

$$CO_2 + H_2O \leftrightarrow HCO_3^- + H^+ \quad (1.2)$$

The bicarbonate then undertakes an acid-base reaction with the amine to yield an overall CO_2 reaction:

$$CO_2 + H_2O + R_2NCH_3 \leftrightarrow R_2NCH_4^+ + HCO_3^- \quad (1.3)$$

Because of that step (carbon dioxide reaction with water to form bicarbonate), it may be assumed that the reaction of H_2S with methyldiethanolamine will be in gas phase limited while the CO_2 reaction is liquid phase limited (Douglas et al. 1987). The rich solution with absorbed H_2S and CO_2 exits the absorber at the bottom and flows into a flash tank. The flash tank is operated at a much lower pressure than the absorber, allowing dissolved light hydrocarbons to be released. Before entering the regenerator, the solution is preheated by heat exchange with the lean solution coming out of the regenerator. In the regenerator, steam generated in the reboiler is used to strip the acid gases from the rich solution.

The regenerated lean amine is then recycled back to the absorber. The gas exiting the top of the reactor is condensed and the steam is recycled to the regenerator as reflux. The remaining acid gas is then sent to flair. From the above description, it can see that GTP is used to remove H_2S and CO_2 in the feed. Depending on the amount of acid gases (H_2S & $CO_{2)}$ present natural gases are classified as sweet gas and sour gas. It is presented in Table 1.1 and 1.2 shows the sour and sweet natural gas reserves around the world.

The gas treatment plant is much more important in the gas processing and refinery operation. The amine plant now attracts increasing attention due to high pressure for environmental compliance and quality of H_2S and CO_2 removal (Hajilary et al. 2011) to prevent corrosion sequences such as:

1- Shutdown of equipment due to corrosion failure.
2- Overdesign to allow for corrosion.
3- Replacement of corroded equipment.
4- Loss of efficiency such as when overdesign and corrosion products decrease the heat transfer rate in heat exchangers.
5- Loss of valuable product, for example, from a container that has corroded through.
6- Inability to use otherwise desirable materials.
7- Damage of equipment adjacent to that in which corrosion failure occurs still other consequences is social.

Corrosion in alkanolamine gas treatment units generally focuses on the cross exchanger's rich side, rich-amine piping after the cross exchanger, the still and the reboiler, where free acid gas and higher temperatures are the main driving forces for corrosion (Dupart et al. 1993). It is not possible to predict with certainty where corrosive attack will take place. Experience has shown that the most likely areas for corrosive attack are those where the temperatures are high, such as in:

- The top part of the still column
- The reboiler tubes
- The heat exchangers
- Some connecting piping

H_2S can cause corrosion in Iron-based metallurgies by forming iron sulfide (FeS),

$$Fe + H_2S \rightarrow FeS + H_2 \quad (1.4)$$

CO_2 also can cause of corrosion problem to form ($FeCO_3$),

$$Fe + CO_2 + H_2O \rightarrow FeCO_3 + H_2 \quad (1.5)$$

Producing in GTP corrosion problems show in next figure.

Figure 1.3. Deposit-covered and corroded rich/lean amine exchanger tubes

Besides, large numbers of technologies are available to measure and controlling corrosion in this kind of units like (NACE 1999):

- Linear polarization Resistance (LPR)
- Electrochemical Techniques
- Mass-Loss Coupons

But due to the fact that this complex is barely new (2 years of operations) there is not available enough expertise and none of those standards mentioned above are also not available in KAR–Khurmala site. So, meanwhile GTP is working blind (no data of corrosion rate in known and no correct action can be taken) to control of this because no any monitoring is available, because of that, this thesis have the motivation to determine the corrosion rate in the unit using analytical techniques by measuring iron content in circulating amine solutions based on fact, more corrosion will dissolve more metallurgical material so, more iron will be liberated to amine stream, if iron concentration can be related with process condition, corrosion rate can be calculated, determined, compared to standards and specification and, of course monitored regularly.

2. LITERATURE REVIEW

2.1. Literature Review Historical Background

According to (Laquai 1988) spectroscopy is an optical instrument that uses for measuring molecular absorption spectra by analyte molecules, usually consists of a source of radiation or lamp, and the optical system that contains a spectral apparatus, a sample compartment, detector and data processing system, data acquisition. Means for amplitude modulation and/or wavelength modulation may also be part of the instrument. Spectroscopy is an important scientific brand that is study dealing with how light or electromagnetic radiation interacts with matter. It is most precise, accurate and powerful equipment that available for analyzing and detecting a small quantity of analyte by the study of atomic and molecular structure. It is an optical system that includes electromagnetic radiation of the region spectrum 100 Å and 400 μm (Behera 2012).

There are as many different types of spectroscopy such as:

2.1.1. X-ray Spectroscopy

X-ray spectroscopy is widely used means of characterizing materials of all forms (Aranaz et al. 2009). There are two main important information of structure that can be obtained by X-ray spectroscopy; electronic structure (deals with valence electron and core electrons, which control the properties of matter chemically and physically. And geometric structure which focus on the information about the arrangement of atoms in a molecule. Many X-ray spectroscopic techniques can be used to obtain electronic and geometric information such as X-ray absorption spectroscopy, X-ray emission spectroscopy, X-ray photoelectron spectroscopy, and X-ray Auger spectroscopy (de Broglie 1913). Due to that flexibility X-ray spectroscopy is a powerful and excellent technique of analysis such as UV-Vis, NMR, IR, and Raman (Lancaster 2011).

2.1.2. Infrared Spectroscopy

Infrared spectroscopy is one of the most important and widely used analytical techniques, the result of this technique depends on the vibrational movement of the atoms of a molecule. The IR peaks is always obtained by passing infrared radiation through a sample that contains a molecules with a permanent dipole moment (Kumirska 2010).

2.1.3. Mass Spectroscopy

Mass spectrometry is one of the important technique that used in the identification process of materials, it is a destructive analytical technique used for measuring the characteristics of individual molecules. The basic information obtained from mass spectrometric analysis is the molecular mass of a compound (De Hoffmann and Stroobant 2007).

2.1.4. NMR Spectroscopy

One of the most powerful techniques for characterizing of a structural and physicochemical study of organic compounds, both small molecules and polymers (Kasaai 2010). There are many other spectroscopic methods applied to the analysis of samples, some of them are combined with flow injection analysis (Pavel, Frantisek and Erust, 1997), Atomic absorption spectrometry and inductively coupled with plasma spectrometry have also been used (Abollino et al 1995). Raman spectroscopy, scanning electron spectroscopy coupled with energy dispersing spectroscopy, Circular Dichroism Spectroscopy.

One of the most important techniques of spectrophotometry is Ultraviolet-visible (UV-Vis) spectroscopy. An equipment which measures the ratio, or function of ratio, of the intensity of two beams of light in the UV-Vis region are called UV-Vis spectrophotometers (Siladitya et al 2012 and Wineland et al. 1987). UV-Vis spectroscopy is useful as an analytical technique for two reasons. Firstly, it can be used to identify certain functional groups in molecules, and secondly, it can be used for assaying. UV-Vis spectroscopy involves the absorption of electromagnetic radiation from the 200–800 nm

range and the subsequent excitation of electrons to higher energy states. This technique can apply for the determination of iron content is amine solution. It includes detecting the amount of UV or visible radiation absorbed by ions of iron Fe^{+2} in the colored amine solution after treatment steps. That optical equipment which measures the amount of UV or visible radiation absorbed by an iron colored solution in UV-Visible region is called UV-Vis spectrophotometers (Hunger and Weitkamp 2001).

In addition, the equipment can take a beam of white light and separate it into its constituent colors (i.e. almost like a prism), therefore the user can study of the absorption of light of individual wavelengths with nearly 1 nm resolution (Hardesty and Attili 2010). The iron content determination in amine solution qualitatively can be done by use of UV-Vis spectroscopy, if we have any data, and quantitative analysis by spectrophotometric is used to ascertain the quantity of analyte that can absorb the electromagnetic radiation. The spectrophotometric technique is easy to use, fast, and almost specific and can be used for small quantities of matter. The basic rule that manages the quantitative analysis by spectrophotometric is the Beer-Lambert law (Gandhimathi et al. 2012). Beer's law: It states that the beam of monochromatic radiation intensity will decrease with increasing number of absorbing molecules. In other words, absorbance is directly proportional and increase with increasing analyte concentration. Lambert's law: It states that the beam of monochromatic radiation intensity will decrease with increasing the thickness of the sample cell. In other words, absorbance is directly proportional and increase with increasing the thickness of the sample cell. So; Beer-Lambert law came from the combination of these two low which state that: When beam of monochromatic electromagnetic radiations passed through a transparent cell that contains a colored solution due to the presence of the absorbing species, the intensity of radiation may occur when some of initial radiation absorbed by the analyte.

Mathematically, Beer-Lambert law is expressed as

$$Abs = \epsilon\, b\, c \tag{2.1}$$

Where, Abs: absorbance by analyte at a specified wavelength, in units of nm for light in the UV-Vis regions of the electromagnetic radiation spectrum; ϵ = extinction coefficient

or absorptivity; b=optical path length of sample cell (cm); c=concentration of Fe^{+2} in solution in unit of molar M; both extinction coefficient (a) and optical path length of sample cell (b) are constant.

Analysis by spectroscopy principle have been created which make utilize both of a reference bend connecting transmittance at a given wavelength with concentration or of the extension coefficient of the colored sample at a given wavelength, a chemical medium that can absorb light should be colored (Basheer et al. 2011). Once it is known the intensity of light after it passes through the cuvette, can be related it to transmittance (T). T is the fraction of light that passes through the sample as shown in the Figure 2.1.

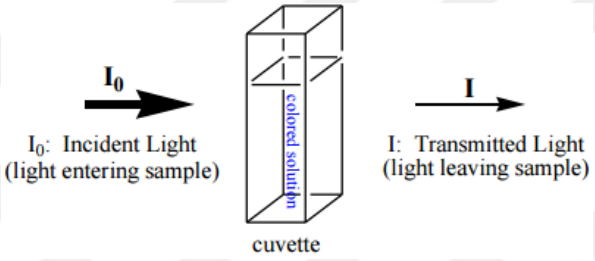

Figure 2.1. Transmittance ($T = I/I_0$) of light by a sample

This can be calculated using the Equation (2.2):

$$T = \frac{I}{I_0} \tag{2.2}$$

Where I is the light intensity after the beam of light passes through the cuvette and Io is the light intensity before the beam of light passes through the cuvette. Transmittance is related to absorption by the expression:

$$\text{Abs} = -\log(\text{T}) = -\log\frac{\text{I}}{\text{I}_0} \tag{2.3}$$

Where, Abs stands for the number or amount of photons that is absorbed by a colored solution of the analyte. With that amount of absorbed photons that calculated from the above equation, the analyte with unknown concentration can be determined by using

Beer-Lambert Law. Figure 2.1 illustrates transmittance of light through a sample (Monica et al. 2012) Beer-Lambert Law (also known as Beer's Law) states that there is a linear relationship between the absorbance and the concentration of a sample (Peter and Julio 2006).

The Beer-Lambert law:

$$\text{Abs} = -\log 10 \frac{I}{I_0} = \varepsilon CL \qquad (2.4)$$

Beer's Law can only be applied when there is a linear relationship Figure 2.2. The method is most often used in a quantitative way to determine concentrations of an absorbing species in solution, using the Beer-Lambert law.

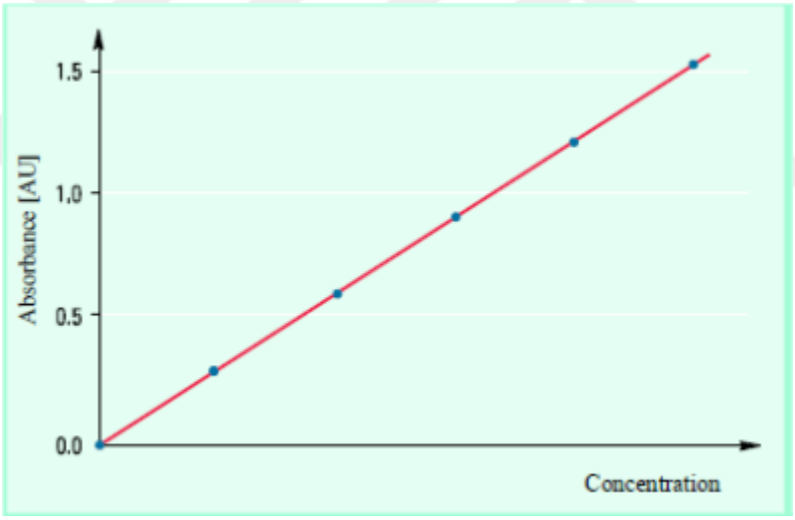

Figure 2.2. Plot of absorbance against concentration

2.2. Determination of Iron Concentration

This study was aimed at determining iron in circulated amine using the proposed molecular absorption spectroscopy method. Iron content is the amount of iron that dissolved in amine solution by corrosion of carbon steel in aqueous rich amine solution by an electrochemical process. The anodic half reaction is the oxidation of iron to ferrous

ion. Fe^{+2} can be determined by reaction with 1,10-phenanthroline compound to form a red-orange colored complex ion. The intensity that complex is measured using a UV-visible spectroscopy (Roy et al. 2009 and Nielsen et al.).

Iron complex is iron (II)-o-phenanthroline, which is orange-red and easy to detect.

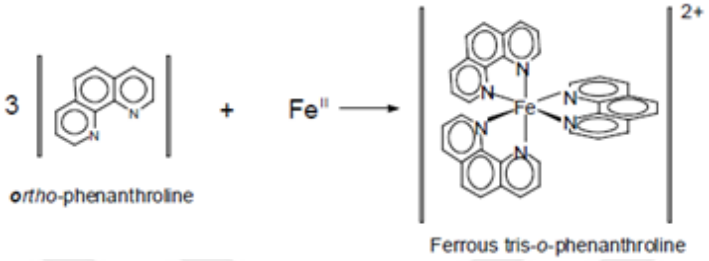

(2.5)

Like most of other metal complexation reactions, the metal ion must compete with hydronium ions; therefore the metal complex will not form strongly acidic medium solutions. And in another hand, insoluble metal hydroxides of most metals can be formed in basic solutions. To prevent the formation of metal hydroxides, the iron determination using o-phenanthroline is carried out in a slightly acidic solution by using 10 mL of concentrated hydrochloric acid 37%. Since it is the ferrous (Fe (II)) called species that forms the reddish-orange complex with o-phenanthroline its structure shown below, a reduction must first be carried out. This can be accomplished.

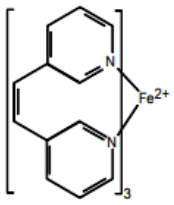

Fe (II)-o-phenanthroline Complex

In this study, you will determine for ferrous Fe^{2+} by reacting with 1, 10-phenanthroline to form a red-orange colored complex ion according to the Equation 2.5. Because corrosions are starting with a Fe^{3+} solution and in order to be quantitative, all of the iron must be reduced from Fe^{3+} to Fe^{2+} by the use of an excess of hydroxylamine hydrochloride.

$$4Fe^{3+} + 2NH_2OH.HCl \rightarrow 4Fe^{2+} + N_2O + 4H^+ + H_2O \quad (2.6)$$

It is not an absolute measurement method. This means that from the signal no direct conclusion on the analyte concentration can be drawn. Therefore, a calibration is necessary which requires standard solutions with known concentrations for creating a calibration curve shown in Figure 2.3.

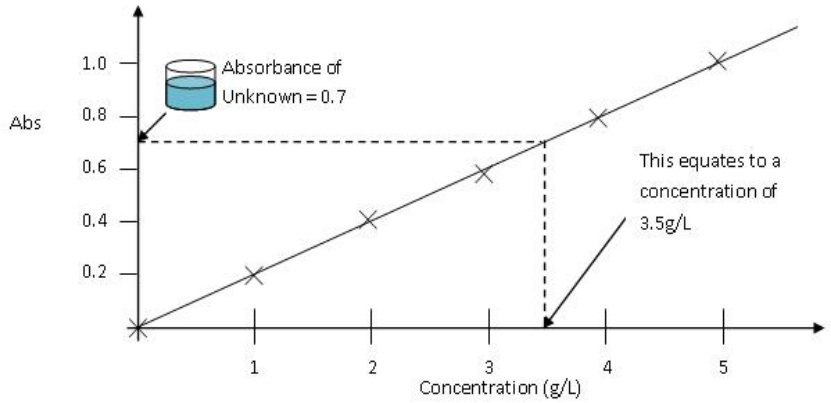

Figure 2.3. Calibration curve for the determination of iron

The determined absorbance was plotted along Y-axis and amount of iron was plotted along X-axis.

2.3. Determination of Corrosion Rate

Iron concentration can be related with process condition, corrosion rate can be calculated, determined, compared to standards and specification and, of course monitored regularly; corrosion in alkanolamine gas treating solutions begins with the acid gases which are the target of the treating, and is enhanced by several physical and chemical factors. Corrosion causes and enhancers are reviewed as are suggestions for mitigating or minimizing corrosive effects (Arthur et al. 2005). Corrosion of metals and their alloys when exposed to the action of acids in industrial processes are recognized as major contributions to infrastructure deterioration. Corrosion is deterioration of metal because of reaction with surroundings. Important types of corrosion are general attack corrosion, metal attack

corrosion, galvanic corrosion, environmental cracking, flow assisted corrosion, intragranular, fretting corrosion and high temperature corrosion (Kulkarni 2015).

Corrosion in circulated MDEA solutions has been studied widely. The reduction of corrosion problem in GTP is much more important and necessary. Most of the investigations have been directed at minimizing corrosion problem of carbon steel, as they are the more extensively used materials in GTP part units (section). Where conditions dictate, also; stainless steels have been used in hotter sections of GTP and acid gas pipes, either where corrosion cannot be controlled otherwise, or where the use of stainless steel would allow greater flexibility in unit operation. When excessive corrosion has occurred, it has often been associated with excessive temperatures and high heat stable acid salt (HSAS) content. Heat-stable amine salts (HSAS) form from stronger acids which can come in from the feed system (2015).

The presence of HSAS reduces acid gas removal capacity, lowers pH, increases conductivity, dissolves protective films and causes corrosion. Velocity accelerated corrosion problem causes erosion by contaminated MDEA solutions containing solid particulates that suspended which remove the protective FeS layer. Corrosion of stainless steel has occurred in reboiler section using high-pressure steam or when upper row tubes become starved and overheated (Addington and Hendrix 2000). The MDEA solution is not naturally corrosive, but corrosion is promoted when absorbed acid gases, higher concentration of corrosive species, higher temperatures, and corrosion on heat transfer Surface higher velocities and HSAS-heat stable amine salts. The HSAS can produce from the amine degradation can also cause corrosion problems. Corrosion in MDEA solution begins with the acid gases which are the target of the treating Amines is compounds formed by replacing hydrogen atoms of ammonia, NH_3 by organic radicals. The chemistry of acid gas removal by amine solutions is relatively complex, but the simplified reactions (exothermic) are (Rennie 2006) as shown form the Equation 1.1 and 1.3. Pure amines are not generally corrosive due to the high alkalinity, but in the presence of acid gases as shown from the above reactions, the corrosivity is largely determined by the stability of protective scales. Corrosion monitoring can be done either by corrosion coupons/probes, or by monitoring iron content in solution, but because of we don’t have technology to do that, iron test is the only option to monitoring of corrosion rate.

Corrosion can occur in alkanolamine gas purification plants. Corrosion in amine plants can be divided into two broad categories:

Wet acid gas corrosion: is the reaction of CO_2 and H_2S with iron through a thin liquid film. If there is a separate aqueous phase and if the only acid gas present is carbon dioxide, the CO_2 will dissolve in the water to form carbonic acid, H_2CO_3. The predominant carbon steel corrosion reaction in wet CO_2 is thought to be the direct reduction of the undissociated acid to form ferrous carbonate (Equation 2.8). Corrosion by acids generally reaction such as:

$$Fe + 2H^+ \rightarrow Fe^{2+} + 2H_2 \quad (2.7)$$

The rate of this corrosion reaction is high depend on the concentration of the hydrogen ions, also this reaction dose happen with carbonic acid, there is also an additional mechanism:

$$Fe + 2HCO_3 \rightarrow Fe^{2+} + 2HCO_3^- + H_2 \quad (2.8)$$

Here the carbonic acid is directly reduced with a rate which also depends on the amount of dissolved. The weak carbonic acid is more corrosive than strong, fully dissociated. The rate of corrosion in steel is very important due to CO_2 is oil and gas industry (Ieaghg 2010). If the acid gas includes hydrogen sulfide, the principal product of corrosion is ferrous sulfide, which is very insoluble, and forms a weakly adherent and somewhat protective iron sulfide film:

$$Fe + H_2S \rightarrow FeS + H_2 \quad (2.9)$$

H_2S can be more corrosive to stainless steel and carbon steel because not only the effect of increasing acidity but also the existence of other localized corrosion mechanisms such as “Sulfide Stress Cracking (SSC)” (Wei and Srdjan 2006). The iron sulfide (FeS) is more protective than iron carbonate ($FeCO_3$), and, if the acid gas contains high amount of H_2S, a protective sulfide film can be formed.

Amine solution corrosion: is the corrosion of carbon steel by aqueous amine. Amine solution corrosion of carbon steel can be caused by a number of factors include:

- High operating temperatures
- High rich and lean amine loadings (moles acid gas/mole amine)
- The ratio of CO_2 to H_2S in the acid gas
- Amine solution contaminants including amine degradation products and heat stable salts.
- Amine solution concentration
- Amine type

Corrosion rate is the speed at which any metal in a particular situation breaks down. It likewise can be characterized as the measure of thickness loose every year by millimeter. The corrosion rate depends on the nature of metals and environment condition. Usually, corrosion rate expressed in mpy (Mils every year) (Wong et al. 2006). The speed or rate of deterioration depends on the environmental conditions and the type and condition of the metal under reference. Determination of corrosion rate in Khurmala GTP is necessary because meanwhile GTP is working blind (no data of corrosion rate in known and no correct action can be taken) to prevent corrosion sequences such as: reduction of metal thickness leading to loss of mechanical strength, hazards or injuries to people arising from structural failure or breakdown, loss of time, contamination of fluids in vessels and pipes loss of technically important surface properties of a metallic component. Mechanical damage to valves and those problems need to consume more money to fix (economic problem). Corrosion can be defined as the destruction of a metal by chemical or electrochemical reactions, or microbial reaction with its environment and Corrosion process in GTP can be explained as the destruction of carbon steel and stainless steel metals by acid gases through electrochemical reactions (Farshad et al. 2010). This impact is evident in equipments made of metals when exposed to corrosion enabling environments, when corrosive reactions occur within or corrosive fluids are transported through or stored in such equipments (Akpa 2013). Many petrol chemical plants such as Khurmala GTP are large-scale equipment, which could be corrosive after some time. Mathematical model to determine the amount of contamination arising from corrosion will have to investigate the deleterious effect of the corrosion on the process of the reaction on the product quality. In corrosion testing, the corrosion rate is measured by the

reduction in weight of a specimen of known area over a fixed period of time. This is expressed by the formula (Oyelami et al.)

$$\text{ipy} = \frac{12w}{tAP} \tag{2.10}$$

Where, w = mass loss in time t/kg; t = time, years; p = density of material, kg/m^3, A = surface area, m^2, in SI units, ipy = 25mm per year.

Corrosion rate expression is readily calculated from the weight loss of the metal specimen during the corrosion test by the formula given below above. Corrosion control parameters significantly affect the corrosion rate and the independently controllable predominant process parameters considered for the investigation are (Suleiman et al. 2013 and Samina et al. 2011): The rate of corrosion increases with increasing the concentration of the acid gases ($H_2S + CO_2$) us shown in the Figure 2.4.

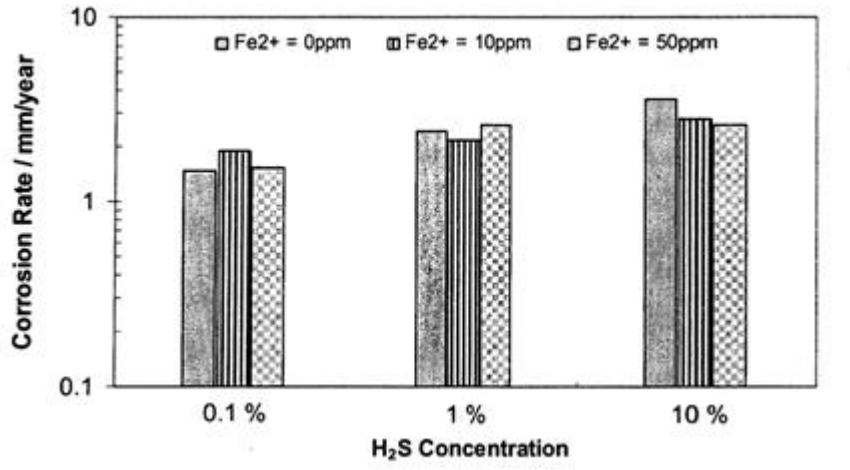

Figure 2.4. The corrosion rate carbon steel at different H_2S concentration and initial Fe^{2+} concentration in the solution with H_2S

The rate of corrosion increases with increase in time and secondly by temperature. Consumption by Hydrogen sulfide (H_2S) in oil and gas industry is an important concern However, H_2S erosion rate, particularly when the pressure and amount of H_2S is high, have not been broadly considered on account of test troubles and related wellbeing issues but we did that due to the lack of corrosion rate detection technology (Navabzadeh and

Nesic 2016). Corrosion phenomena is occur electrochemically, and electrochemical system is expected to think about the information picked up by measuring mass changes in the oil and gas industry after some time. The electrochemical technique can be used to measure corrosion rate through polarization estimations. The primarily preferred standpoint of such an estimation is, to the point that individual anodic and cathodic responses occurring. What's more, the corrosion current (and thus the consumption rate) can be dictated by extrapolation of the cathodic or anodic Tafel lines on a polarization plot of the corrosion potential (E_{corr}). This is then embedded into Faraday's Law (Gray et al. 2005):

$$Corrosion\ Rate\ (\frac{mols}{S}) = \frac{\text{I corr}}{\text{n}*\text{F}} \quad (2.11)$$

Where, n = number of electrons involved in the reaction; F = Faraday's constant = 96.500 A/s (Coulombs). This is then converted to mass gain/second by the relationship between moles and mass: mass of sample = moles * molecular mass of compound

There are three main methods that are used to express the corrosion rate:
a) Thickness reduction of the material per unit time.
b) Weight loss per unit area and unit time.
c) Corrosion current density.

Thickness lessening per unit time is the measure of most functional hugeness and intrigue. In the Metric framework, this measure is generally expressed in mm/year. In some writing, one can even now discover the unit mils every year (mpy) = 1/1000 inches per every year, perhaps at the same time inches per every year (ipy). Weight reduction per unit area and unit time was ordinarily utilized as a part of prior circumstances, for the most part since weight reduction was typically the directly decided amount in corrosion testing. Here the test examples were weighed prior and then afterward the presentation to the corrosion medium. On this premise, one could ascertain the thickness decrease as weight reduction per unit area /density.

Figure 2.5 explained that corrosion rate also can be expressed by corrosion current density. The dissolution rate (the corrosion rate) the metal ions that loss per unit area over the time passed (Einar 2004).

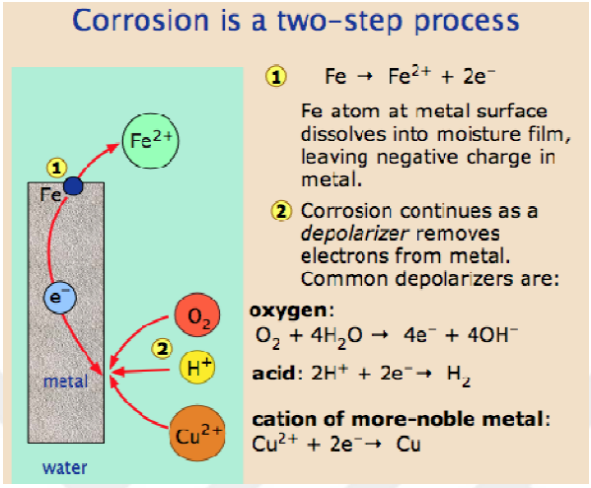

Figure 2.5. Electrochemical corrosion of iron

The relationship between thickness reduction per time unit ds/dt (on each corroding side of the specimen/component) and the corrosion current density Icorr is determined from Faraday's equations: $\frac{ds}{dt} t \frac{icorr}{2FP} \frac{cm}{s}$ or $\frac{\Delta s}{\Delta t} t3268 \frac{\text{icorrM}}{\text{ZP}}$ mm/year. The Butler-Volmer relationship for current density depends on the recognizing the anodic and cathodic responses that are occurring on every electrode. In any condition, a metal is experiencing both an anodic and a cathodic response. This trademark is the thing that requires the net current density to represent the two responses on each metal, the metal is going about as the anode or the cathode in a galvanic couple. At the zero overpotential, the anodic and cathodic current is equivalent; this point is known as the current exchange. In any case, when the overpotential isn't equivalent to zero, the anodic and cathodic current is unique.

Therefore, for a given electrode, the anodic current density is $i_{anodic} = i_0 \exp\left[a_{anodic} \frac{zF(\phi-\phi_0)}{RT}\right]$ while the cathodic current density is $i_{cathodic} = -i_0 \exp\left[-a_{cathodic} \frac{zF(\phi-\phi_0)}{RT}\right]$. So that net current density is $i_{net} = i_{anodic} + i_{cathodic} = i_0 \exp\left[a_{anodic} \frac{zF(\phi-\phi_0)}{RT}\right] - i_0 \exp\left[-a_{cathodic} \frac{zF(\phi-\phi_0)}{RT}\right]$. This is

known as the Butler-Volmer equation. Hence, for Electrode A, which acts as the cathode, the total current density is $i_A = i_{0,(A)}\left[\exp\left(\frac{\mathrm{a}_{a,A}zF(\phi-\phi_{0,(A)})}{RT}\right) - \exp\left(\frac{-\mathrm{a}_{c,A}zF(\phi-\phi_{0,(A)})}{RT}\right)\right]$. For electrode B, which acts as the anode, the total current density is $i_B = i_{0,(B)}\left[\exp\left(\frac{\mathrm{a}_{a,B}zF(\phi-\phi_{0,(B)})}{RT}\right) - \exp\left(\frac{-\mathrm{a}_{c,B}zF(\phi-\phi_{0,(B)})}{RT}\right)\right]$. At low overpotential, (ϕ-ϕ_0) <0.01V, the Butler-Volmer equation reduces to the following linear relationships for current density-potential; cathodic, $i_A = \frac{i_{0,(A)}zF(\phi-\phi_{0,(A)})}{RT}$, anodic, $i_B = \frac{i_{0,(B)}zF(\phi-\phi_{0,(B)})}{RT}$. On the other hand, at large overpotential an exponential (Tafel) relationship results. For anodic polarization (ϕ-ϕ_0)>0.01V, the Butler-Volmer equation reduces to $i_{net} = i_0\exp\left[\mathrm{a}_{anodic}\frac{zF(\phi-\phi_0)}{RT}\right]$. Such that the expression for the overpotential is $(\phi-\phi_0) = \alpha\log_{\mathrm{e}}\frac{i_{net}}{i_0}$. This is known as the anodic Tafel equation. For cathodic polarization (ϕ-ϕ_0) <-0.01V, the Butler-Volmer equation reduces to $i_{net} = -i_0\exp\left[-\mathrm{a}_{cathodic}\frac{zF(\phi-\phi_0)}{RT}\right]$. Such that the expression for the overpotential is $(\phi-\phi_0) = \beta\log_{\mathrm{e}}\frac{i_{net}}{i_0}$. This is known as the cathodic, Tafel equation. The relationships that were used to determine the appropriate transfer coefficients are $\mathrm{a}_{anodic} = \frac{RT}{zF\alpha}$ and $\mathrm{a}_{cathodic} = \frac{RT}{zF\beta}$. Regardless of the relationship used for the current density, the flux source boundary condition reflects the relationship in Equation for the surfaces of electrode A and electrode B respectively. $\frac{\partial\phi}{\partial n} = \frac{\partial\phi}{\partial y} = \frac{-i_{A\ or\ B}}{\sigma}$, where y is the distance from the electrode surface.

The Nernst equation is an equation In electrochemistry can be explain as the reduction potential of an electrochemical reaction to the standard electrode potential, temperature, and activities (often approximated by concentrations) of the chemical species undergoing reduction and oxidation. The relation is affected by temperature and whether the membrane is more permeable to one ion over others (Bagotsky S., 2006). The equation may be written: $E_{cell} = E^0_{cell} - \left(\frac{RT}{nF}\right)lnQ$, where: $\mathrm{E}_{\mathrm{cell}}$ = cell potential (V); $\mathrm{E}^0_{\mathrm{cell}}$ = cell potential under standard conditions; R = gas constant, which is 8.31 (volt-coulomb)/ (mol-K); T = temperature (K); n = number of moles of electrons exchanged in the electrochemical reaction; F = Faraday's constant, 96500 coulombs/mol; Q = reaction quotient, which is the equilibrium expression with initial concentrations rather than

equilibrium concentrations. Sometimes it is helpful to express the Nernst equation differently: $E_{cell} = E^0_{cell} - \left(2.303 * \frac{RT}{nF}\right) \log Q$. The important specifications in GTP are the amount of acid gas content. Alkanolamine solution (MDEA) has been considered the best chemical to removing H_2S gas from natural gas. It is depend on the reaction of a weak base (MDEA) and a weak acid (acid gas or H_2S) to produce a water-soluble amine acid gas salt called rich amine. For diethanolamine, the reaction can be stated as (Zare and Mirzaei 2009). $[Amine] + H_2S = [Amine]H^+HS^-$, this reaction creating the rich amine and can be reversed under certain temperature in regeneration system, which allows the amine to be regenerated and recycled to the contactor for additional acid gas removal the amount of acid gas bonded to the amine is called the rich loading. Given the right conditions, amines can load up with so much acid gas the solution becomes corrosive and causes problems and inefficiencies in the heat exchanger. Overloading the amine usually results from under circulating the solution. Under loading the solution is a more common problem, and is a result of over circulating the amine (West 2008).

Acid gases in amine plant included CO_2 and H_2S: $CO_{2_g} \leftrightarrow CO_2$ and $H_2S_{(g)} \rightleftharpoons H_2S_{(liq)}$. Liquid solutions we have rich amine/lean amine, acid gases are sour gas/sweet gas. Depending on site could be: 1st pair: sour gas/rich amine and 2nd pair: sweet gas/lean amine. Applying Henry law: $[CO_2]_= f\ CO_{2\ (gas)} / H_{CO2}$ and $[H_2S]_= f\ H_2S_{(gas)} / H_{H2S}$. Where: f= Fugacity; H=Henry constant. 1st step: determine if binary system is working at steady Henry law and fugacity law how? Comparing fugacity: 2nd step equilibrium state maths: $CO_2 + H_2O \leftrightarrow H_2CO_3$; dissiociation of H_2CO_3, K_1; $H_2CO_3 \leftrightarrow H^+ + HCO_3^-$ ... K1; Dissociation of HCO_3^-, K_2; $HCO_3^- \leftrightarrow H^+ + CO_3^{2-}$ ... K2; and for H_2S, K_3; $H_2S \leftrightarrow H^+ + HS^-$ ... K3; Dissiociation of HS^-, K_4; $HS^- \leftrightarrow H^+ + S^{2-}$ ... K4; at water occure also: $H_2O \leftrightarrow H^+ + OH^-$ ... KW. Equilibrium conatant for carbonic acid can be written as: $K_1 = \frac{[H^+][HCO_3^-]}{[H_2CO_3]}$ and $K_2 = \frac{[H^+][CO_3^{-2}]}{[HCO_3^-]}$. Equilibrium constant for carbonic acid can be written as: $K_3 = \frac{[H^+][HS^-]}{[H_2S]}$ and $K_4 = \frac{[H^+][S^{-2}]}{[HS^-]}$. For H_2O: $K_w = [H^+][OH^+]$, 3rd step: component balance, for carbon: $[CO_2]_{liq} = [H_2CO_3]_g + [HCO_3^-] + [CO_3^-]$, for H_2S will be: $[H_2S]_{liq}[H_2S]_g + [HS^-] + [S^{2-}]$.

Applying electroneutrality: $[H^+] - [HCO_3^-] - 2[CO_3^{2-}] - [OH^-] - 2 - [S^{2-}] - [HS^-] = 0$. 4th step: determination of corrosion reaction mechanism; anodic reaction, $Fe \rightarrow Fe^{2+} + 2e^-$ and cathodic reactions: $2H_2CO_3 + 3e^- \rightarrow 2H + 2HCO_3^-$; $2HCO_3^- + 2e^- \rightarrow H^+ + 2CO_3^{2-}$; $2H_2S + 2e^- \rightarrow H^+ + 2HS^-$; $2HS^- + 2e^- \rightarrow H^+ + 2S^{2-}$; $2H^+ + 2e^- \rightarrow H_2$.

Bolter-Volmer equation (electrochemical kinetics):

$$i = i_0 \left[\exp\left(\frac{\alpha_a z F \eta}{RT}\right) - \exp\left(-\left(\frac{\alpha_c z F \eta}{RT}\right)\right)\right] \quad (2.12)$$

Where: i =current density (A/m^2); i_0 =current density (A/m^2); T=absolute temperature, K; Z= number of electrons involved in the electrode reaction; F= Faraday constant; R=Universal gas constant; $\alpha_{c=}$ cathodic charge transfer coefficient, dimensionless; α_a = anodic charge transfer coefficient, dimensionless; η= activation overpotential, defined as: E=Electrical Potential, V, $\eta = (E - E_{eq})$; E_{eq}=Equilibrium Potential, V.

Appling Volmer:

$$i_{H2CO3} = i_0\ H_2CO_3.\exp = \frac{2\alpha F \eta H2CO3}{RT} \quad (2.13)$$

$$i_{0\ H2CO3} = 2FKe\ H_2CO_3\ [H_2CO_3] \quad (2.14)$$

$\eta H_2CO_3 = E_{corr}$ -E $_{H2CO3}$; substitution of Equations 2 and 3 in Volmer equation: $i_{H2CO3=}$2FKe H_2CO_3 $[H_2CO_3]$. $\exp[\frac{-\alpha F(Ecorr - E\ H2CO3\ )}{RT}]$, for other species will be: $i_{HCO3-=}$2FKe HCO_3^- $[HCO_3^-]$. $\exp[\frac{-\alpha F(Ecorr - E\ HCO3-\ )}{RT}]$; $i_{H2S=}$2FKe H_2S $[H_2S]$. $\exp[\frac{-\alpha F(Ecorr - E\ H2S\ )}{RT}]$; $i_{HS-=}$2FKe HS^- $[HS^-]$. $\exp[\frac{-\alpha F(Ecorr - E\ HS-)}{RT}]$; $i_{H+=}$2FKe H^+ $[H^+]$. $\exp[\frac{-\alpha F(Ecorr - E\ H+)}{RT}]$; $i_{Fe=}$2FKe Fe [Fe]. $\exp[\frac{-\alpha F(Ecorr - E\ Fe)}{RT}]$ and

$$Ke = 10^{((A/T)-B)} \quad (2.15)$$

A and B coming from Tafel equation: A= (0.059/ αn) ln j_0 and B= (0.059/ αn) = 2,303RT/αF. And the equilibrium constant by Nernst law:

$$E = E^0 + \frac{RT}{NF} Ln \frac{[OH]}{[Red]} \quad (2.16)$$

So; $i_{H_2CO_3} + i_{H_2S} + i_{HS^-} + i_{H^+} + i_{Fe} + j_{HCO_3^-} = i_{corr}$, then: $(mpy) = \frac{i_{corr}\ total\left(\frac{amp}{cm^2}\right) * F}{\rho Fe, cast\ alloy. Peq}$; $(mpy) = i_{corr}. 4.6 * 10^{5^-}$. Then with (mpy) related with gradient Fe, H_2S loading:

$$mpy = \frac{Kai}{nD} \quad (2.17)$$

Where, a=atomic weight; i =current density; n=number of electron lost; D=density of metallic; K=3.2 K.

3. MATERIALS AND METHODS

3.1. Materials and Equipments

3.1.1. Chemicals

Purity of reagents-reagent grade chemicals shall be used in all tests. Unless otherwise indicated, it is intended that all reagents shall conform to the specification of the committee on analytical reagents of the American Chemical Society, where such that the reagents is sufficiently high purity to permit its use without lessening the accuracy of the determination. Chemicals that use in this study are shown in the Table 3.1.

Table 3.1. List of chemical reagents

Reagent	**CAS number**	**Company**
Ammonium acetate HPLC grade >99.0%.	631-61-8	SIGMA-ALDRICH
Hydroxylamine hydrochloride 99.0%.	5470-11-1	SAMCHUN
1, 10 Phenanthroline-monohydrate 99.5%.	1.07225.0010	MERCK
Iron standard solution 1000mg/L Fe for AA (Iron (III) nitrate nona hydrate in nitric acid 0,5 mol/L.	HI03020100	Scharlau
Nitric acid 65% analytical grade.	1.00556.2500	MERCK
Iodine Crystal 99%	7553-56-2	SIGMA-ALDRICH
Lead(II) Acetate trihydrate 99.5 -102.0 %	A6094421 401	MERCK
Starch analytical grade	AL07150500	Scharlau
Salicylic Acid extra pure 99 – 101 %	AC20020500	Scharlau
Hydrochloric acid fuming 37%	K44134417	MERCK

3.1.2. Instruments and Apparatus

Table 3.2. List of instruments and equipments

Equipments and Instruments	Technical specification	Brand
Spectrophotometer	EMC-11-UV (UV-1100)	
	S/N: 130849	EMC LAB
Auto Titrator	10 Titra (K90590)	
	S/N:B262013020	Koehler
pH meter	HI 2211	HANNA
	PH/ORP	
Electronic balance	220 g capacity (No.WB1310163)	
	Type: ABS 226-4	KERN
Micropipette	100-1000µl	Dragon
	YE5E508709	Lab
DIGITRATE	S/N AF5789	ISO lab

3.2. Procedures and Techniques

In this section is explained the detailed procedures used to determine the analytes: H_2S loading, iron content and concentration of MDEA in the sweetening solvent at samples taken during sampling procedures.

3.2.1. Determination of Iron in MDEA Sweetening Solvent

Procedure is as follows: shake the sample to be homogenized. Using 25 ml capacity cylinder to take amine sample then transfer into 100 ml capacity beaker, if the sample contains more than 200 µg iron and use a smaller aliquot and dilute to 50 mL with distilled water. Figure 3.1 show us first step.

Figure 3.1. 25 ml sample with 10 ml HCl

Simultaneously prepare a reagent blank sample using distilled water. Add 10 mL of HCl concentrated, mix well wait until reaction's consumption. Heat the mixture using hot plate until fumes occur, boils slightly and allow five minutes after confirming the disappearance of H_2S vapors using H_2S sensing paper. Caution: this operation must be done in fume hood. For rich amine the stripping of H_2S could take longer. The tone of the paper should not change in the last two measurements as shown in the Figure 3.2.

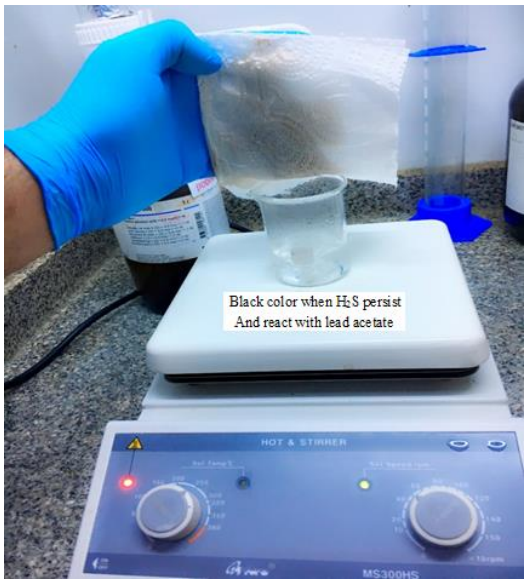

Figure 3.2. H_2S detection by lead acetate

Remove from heat, expect cool, and add 1 mL of solution hydroxylamine hydrochloride 10% mix. Heat the mixture again and wait until the volume is reduced by half, as shown in the Figure 3.3.

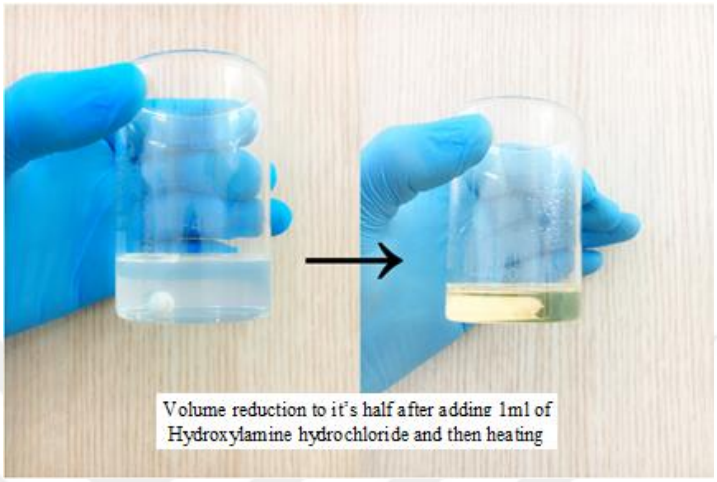

Figure 3.3. Volume reduction to half

Let cool to analytical room temperature. Caution: the precision depends at control room's temperature to form the iron complex. Keep the air conditioner at 25 C with no air draft-free. Add 10 ml of ammonium acetate buffer. Homogenize. Verify that the pH is between 2.5 to 5 using pH meter or pH sensing paper. Add 4 mL of phenanthroline solution. And intense red-orange color produced, as shown from Figure 3.4.

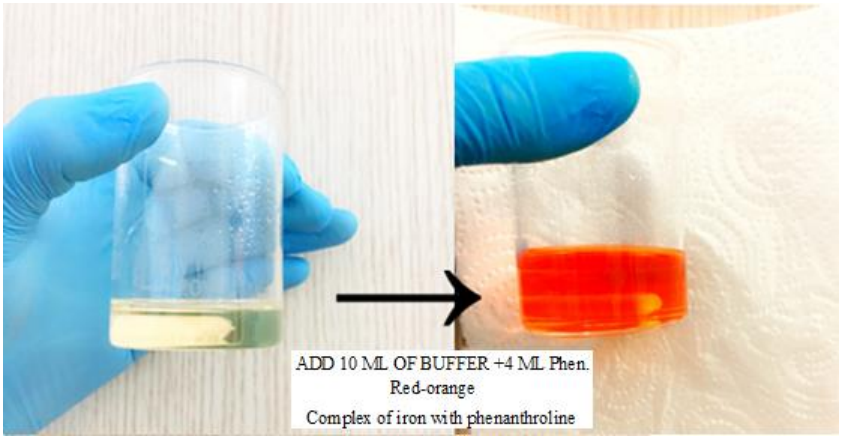

Figure 3.4. Color change after chemical addition

Quantitatively transfer the mixture from the erlenmeyer or beaker to a volumetric flask 50 or 100 mL capacity. (The volumetric flask must be previously clean. Remember that cleaning must be free of metals). Make up volume with iron free water, as shown from Figure 3.5. Homogenize and leave to develop color for half an hour. If the solution is haze filter a portion necessary to analyze.

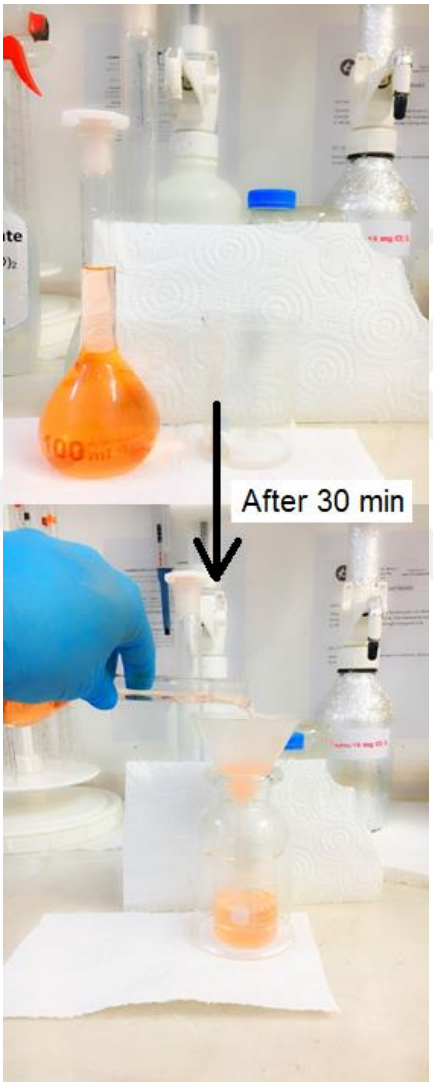

Figure 3.5. Filtration of sample

Proceed to read the concentration of iron using a cell of 1 cm quartz following with UV-1100 Spectrophotometer. Figure 3.6 show that if the absorbance is higher than 0.4 dilute to get a value into the calibration curve.

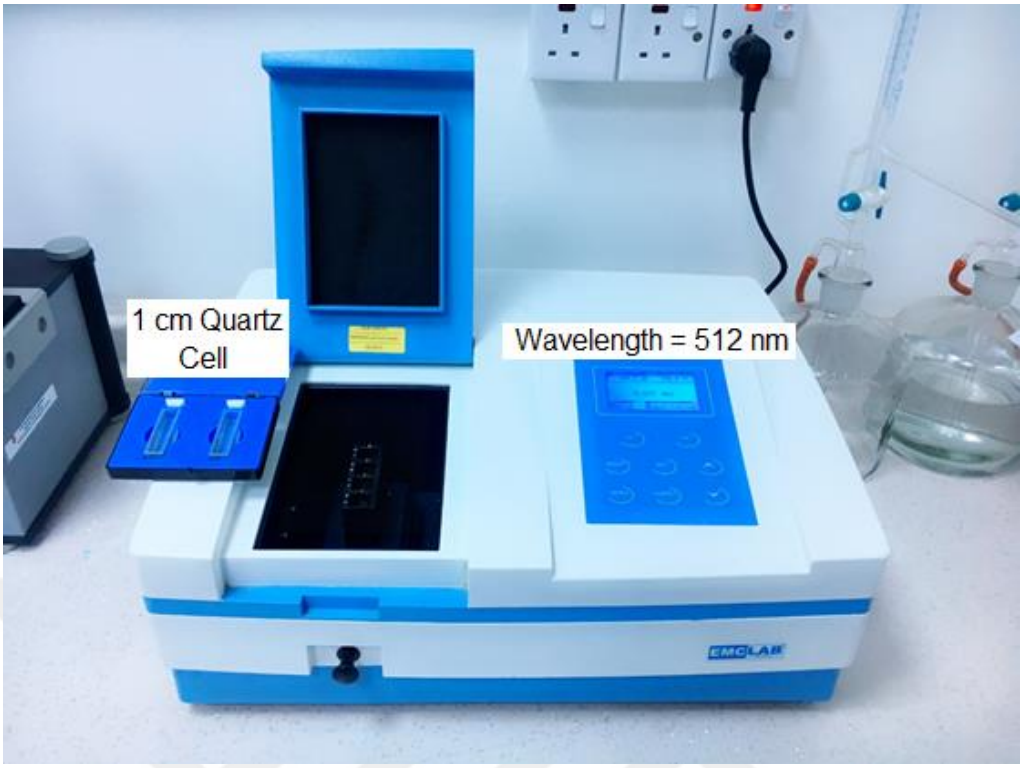

Figure 3.6. UV-1100 Spectrophotometer

3.2.2. Determination of MDEA Concentration

This test method describes the steps used for determination MDEA concentration in samples of lean amine and rich amine by potentiometric method titration with 0.5 M HCl, there is an important parameter of control of GTP. MDEA: methyldiethanolamine, chemical substance utilized like sequestrate of H_2S and CO_2 in the sour gas, allowing controlling the efficiency of the unit of treatment of gas minimizing the emission of oxides of sulfur to the atmosphere. Interferences: the ammonia high content in the sample may provide wrong result. Summary: a portion of the sample to be examined is dissolved in deionized water itself and is titrate with standard HCl potentiometrically by AUTO-TITRATOR instrument.

Steps: a) weight in a beaker between 0.2 to 0.5 grams of sample as shown in Figure 3.7.

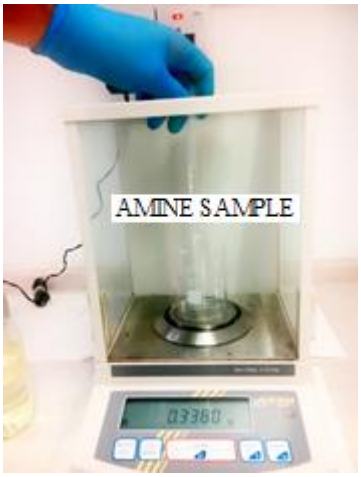

Figure 3.7. Weighing sample by analytical balance

b) Dissolve the sample into 100 ml of water as in Figure 3.8.

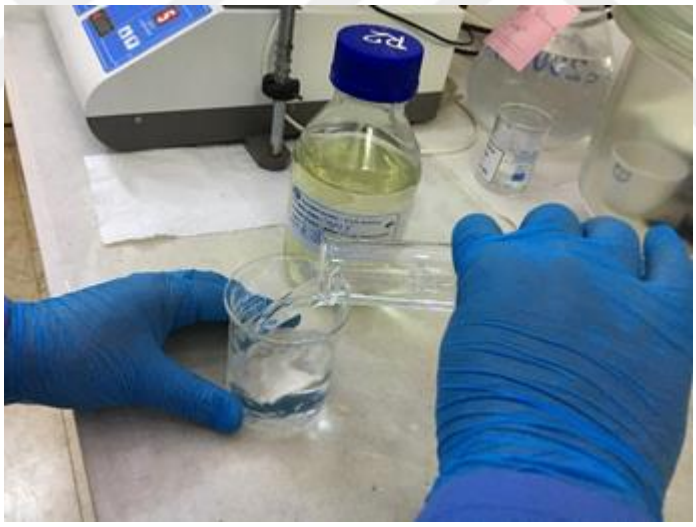

Figure 3.8. Sample dissolving with 100 mL of distilled water

c) Place the diluted sample in titration cell (100 mL) wait for test development (Figure 3. 9).

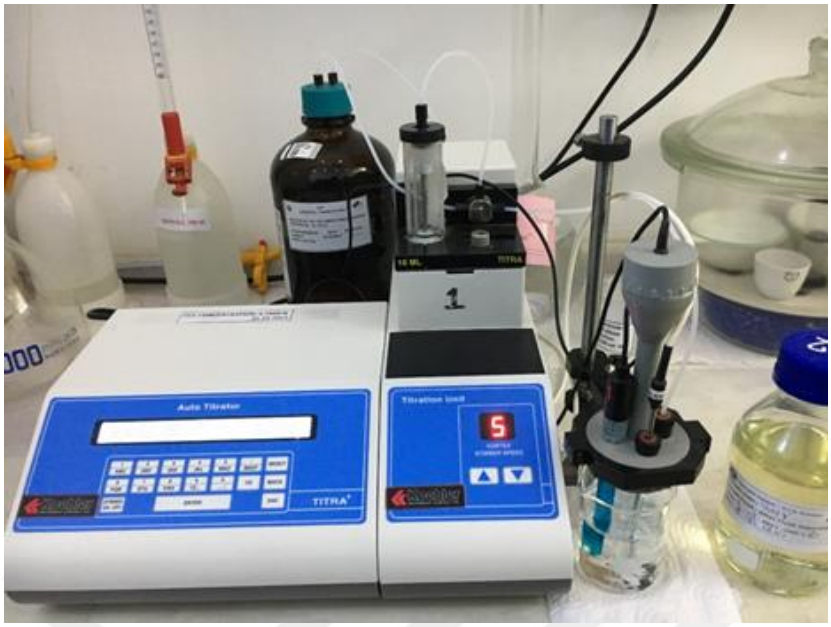

Figure 3.9. Sample run with auto titrator

d) Record the spend volume and calculate the concentration as the follow:

Experimental Data: V_{HCl} spent=2.413 mL (V1), N_{HCl}=0.5 N (N_{HCl}), weight of sample =0.298 g (Ws), volume of blank =0.02 mL (V_B). Equation: MDEA concentration = $\frac{(V_{HCl}-V_B)*N_{HCl}*119}{W_s} = \frac{(2.413mL-0.02mL)*\left(\frac{m\,eq}{ml}\right)*119}{0.298\,g}$; MDEA conc.=46.887 ~ 46.9 % w/w.

3.2.3. Apparent H_2S in Amine Solution

A control and precision method are used for the determination of apparent hydrogen sulfide in amine solution. Hydrogen sulfide is determined by oxidation with standard iodine solution in acidic medium. If thiosulfate is present, is also titrated an included H_2S in the calculation. Thiosulfate maybe determined by UOP method 827, and the value thus obtained substrate from apparent H_2S concentration the lower limit of detection is approximately 25 grains/gallon.

Summary: control method; for a plan control work with lean amine containing of level of hydrogen sulfide. Direct titration maybe used. Apportion of amine sample is pipettes into water acidify with concentrated HCl, and immediately titrated with standard iodine

solution using starch as the indicator. Precision method: for a solution containing more than 100 grain of H_2S per gallon or where better precision is required. Portion of amine sample is pipette into an acidic water solution containing an excess standard iodine solution. The excess of iodine is back titrated with standard sodium thiosulfate solution using starch as indicator.

Steps to analyze H_2S in MDEA solvent: a) Arrange the apparatus in an efficient hood to avoid any hazard from the evaluation of gaseous H_2S. b) Determination the amount of sample to be taken for analysis from the following Table 3.1:

Table 3.3. Amount of sample according H_2S concentration

Apparent H_2S concentration expected in the sample grain/gallon	Sample size mL
>100	1.0
<100	5.0 – 10.0

c) Pipette appropriate size sample into a 250 mL erlenmeyer flask containing a magnetic stirring bar and 100 ml of water with viscous sample, rinse the pipette with water and add the rinsing into the flask. d) Pipette a volume of HCl, equal to the sample size taken into the flask. e) Add approximately 2 mL of starch indicator solution.as shown form below Figure 3.13.

Figure 3.10. Mixture of sample with HCl ready for titration

f) Turn on the magnetic stirrer and titrate immediately with standard 0.05 M iodine solution until a deep-blue color persists as in Figure 3.11.

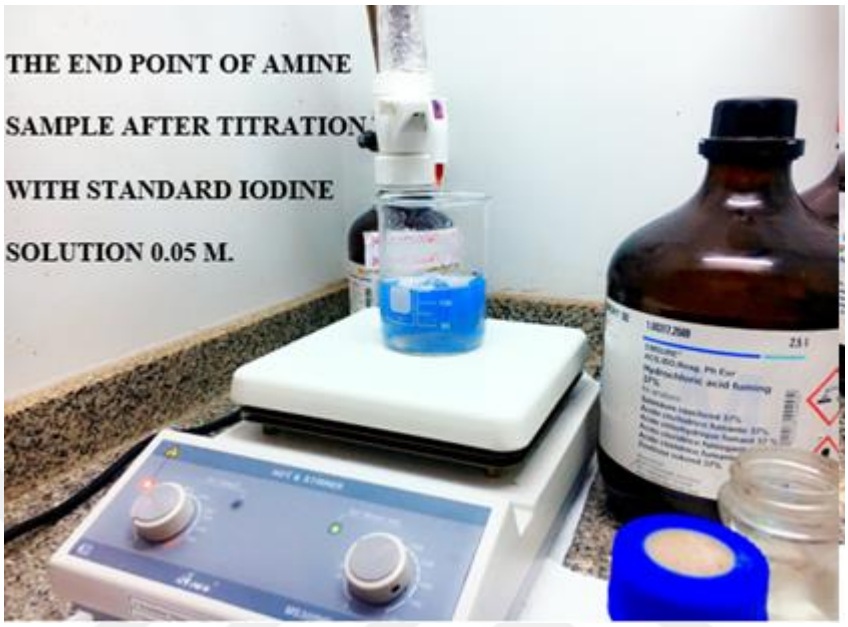

Figure 3.11. End point

g) With the spend Iodine solution volume and sample's volume proceed to calculate H_2S loading as in the following calculation.

Calculation of H_2S loading at 39095 ppm and Amine concentration of 46.9% in sweetening solvent: Part one; H_2S loading at 39095 ppm, experimental data; volume of IO_3/I_2 spent =4.81 (V_{I2}); molarity of standard iodine solution =0.05M (M_{I2}); volume of sample 0.2 mL (V.s); specific gravity =1.042 (S.g); equations: $H_2S\ loading = \frac{(V_{I_2} * M_{I_2} * 1991)}{V.S}$; $H_2S\ loading(ppm) = \frac{17 * H_2S\ loading\left(\frac{grain}{gallon}\right)}{S.g}$. Combining both equations: $H_2S\ loading = \frac{V_{I_2} * M_{I_2} * 1991 * 17}{V_S * S.g} = \frac{4.81mL * 0.05\ m\ mole * 1991 * 17}{0.2\ mL * 1.042}$ = 39095 ppm-w.

4. RESULTS AND DISCUSSION

In this section of the research results and explanations concerning how the corrosion rate in GTP was estimated using analytical determination of iron released into MDEA solvent during process. The results are presented for each objective achieved in research, in details are presented as: a) validation of iron determination by molecular absorption spectroscopy; b) results of iron, MDEA concentration and H_2S Loading over a set of samples at scope of this study, c) estimation of corrosion rate based on Volmer, Tafel and Nernst laws, d) evaluation of results by comparison of corrosion rate with standards specifications or typical data of corrosion rate in this kind of systems.

4.1. Validation of Iron Determination by Molecular Absorption Spectroscopy

In this section is presented the results of calibration of UV spectrophotometer, in this order of ideas, before reading any standards were necessary to determine the optimal analytical wavelength a graph of absorbance vs λ (nm) is presented in Table 4.1 and Figure 4.1 and after plotting those experimental data can be seen the absorption molecular graph of iron-phenanthroline optical active compound.

Table 4.1. Absorbance of 0.7µg Fe at different wavelength

Wavelength(nm)	Absorbance of 0.7 µg Fe standard
495	0.085
500	0.092
505	0.11
510	0.13
512	0.14
515	0.135
520	0.122
525	0.113
530	0.10
535	0.085
540	0.067

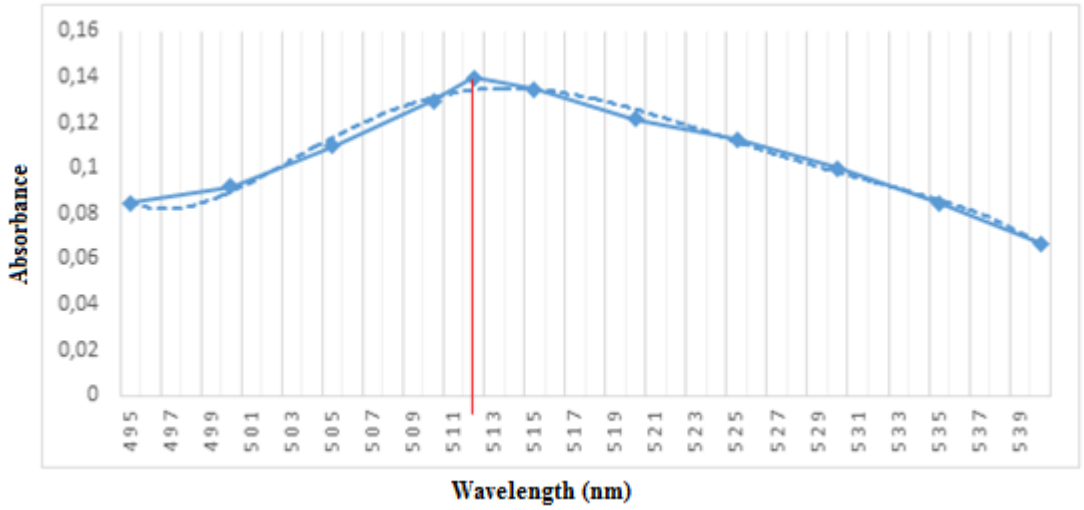

Figure 4.1. Determination analytical wavelength

As can be observed, at 512 nm with a threshold of 0.1 nm is achieved maximum absorption, the maximum molecular absorption coefficient is at this wavelength, because of this, and the calibration curve was settled down at these experimental conditions:

- Analytical λ = 512 nm
- Threshold = ± 0.1 nm (spectrophotometer resolution)
- Temperature = 25 C.
- Atmospheric pressure: 1008 mBar.
- Optimal media: quarts cells – 1 cm path.
- Matrix: MDEA 50%.

After determinate these optimal conditions, calibration curve was done reading standards and making statistical regression for linear type calibration. Table 4.2 shown results of average absorbance for each standard and the calibration curve obtained.

Table 4.2. Absorbance of standard sample at λ=512 nm

Standard Concentration, ppm	Absorbance λ=512 nm
0	0
0.4	0.081
0.8	0.165
1.2	0.257
1.6	0.335
2.0	0.401

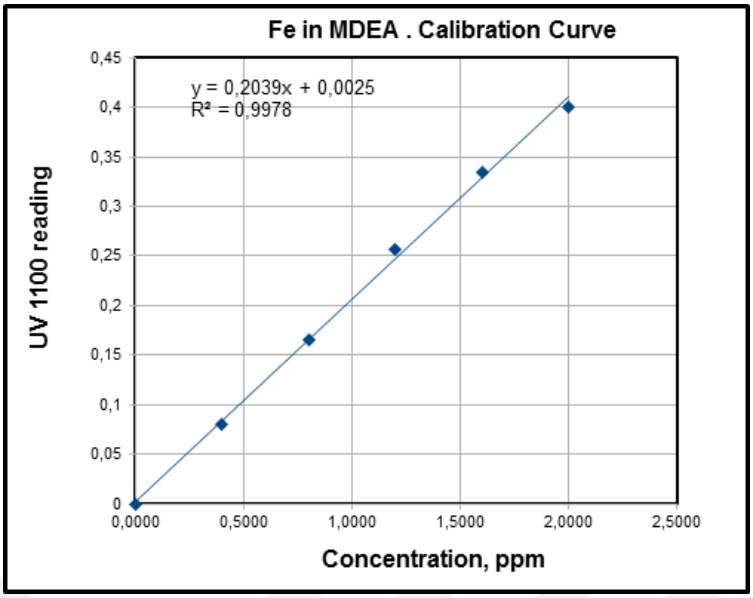

Figure 4.2. Calibration curve between concentrations of standard with absorbance

After calibration, statistical results show a linear regression coefficient of 0, 9978 and a relative error of 2.35%. With these results can be declared a validated calibration because the minimum value of R^2 is 0.990 to be allowed as acceptable, also relative error must be less than 5% to achieve validation condition. This fact can be observed at comparison of calibration validation parameters vs. acceptance criteria (Table 4.3).

Table 4.3. Validation parameters for Fe calibration in MDEA

Validation parameters	Values	Acceptance Criteria
# of standards	5	Min. 3
# of lectures by standard	3	Min. 2
Linear regression Coefficient	0.9978	Min. 0,990
Calibration Standard Deviation,%	0.08	Max. 5%
Error, %	2.35	Max 5%
Regression equation	Y=0.2039X + 0.0025	Linear

X: concentration of Fe, ppm; Y: absorbance

4.2. Results of Iron, MDEA Concentration and H_2S Loading

In this section can be observed the results concerning to sampling schedule applied as a Table 4.4.

4.2.1. Iron Content in Rich Amine Solution

Table 4.4. Iron content at rich amine samples sampled in July/August

Date	Iron content/ppm	Date	Iron content/ppm
1-July	1.62	31-July	1.23
2-July	0.77	1-August	0.59
3-July	1.37	2-August	2.71
4-July	0.73	3-August	0.93
5-July	0	4-August	0.77
6-July	0.93	5-August	0.91
8-July	0.93	6-August	0.91
9-July	0	7-August	1.01
10-July	1.87	8-August	0.94
12-July	0.73	9-August	1.54
13-July	0	10-August	1.21
25-July	1.09	11-August	1.08
26-July	2.71	12-August	0.77
27-July	3.11	13-August	0.97
28-July	3.03	14-August	0.91
29-July	2.11	15-August	1.06
30-July	1.54		

4.2.2. Rich Amine Concentration

Table 4.5. Concentration at rich amine samples sampled in July/August

Date	[Rich amine]%	Date	[Rich amine]%
1-July	46.9	31-July	50.1
2-July	46.7	1-August	49.4
3-July	46.1	2-August	----
4-July	47.7	3-August	49.5
5-July	47.6	4-August	49.2
6-July	----	5-August	48.8
8-July	47.1	6-August	48.5
9-July	48.2	7-August	49.6
10-July	47.2	8-August	49.3
12-July	47.5	9-August	49.4
13-July	47.5	10-August	49.1
25-July	47.2	11-August	49.1
26-July	47.9	12-August	48.6
27-July	47.8	13-August	48.7
28-July	48.1	14-August	48.7
29-July	48.3	15-August	48.9
30-July	50.1		

--- No data available

4.2.3. H_2S Loading

Table 4.6. H_2S loading at rich amine samples sampled in July/August

Date	H_2S loading/ppm	Date	H_2S loading/ppm
1-July	39095	31-July	39136
2-July	38863	1-August	39241
3-July	37511	2-August	39624
4-July	38438	3-August	39868
5-July	38515	4-August	52886
6-July	---	5-August	37183
8-July	39288	6-August	-----
9-July	37125	7-August	39827
10-July	44628	8-August	39664
12-July	37386	9-August	39176
13-July	37671	10-August	38322
25-July	38525	11-August	39195
26-July	54513	12-August	36541
27-July	55042	13-August	36613
28-July	53373	14-August	33277
29-July	51915	15-August	37630
30-July	43529		

4.3. Estimation of Corrosion Rate Based On Volmer, Tafel and Nernst Laws Using Iron Content

4.3.1. Conversion of Iron Content

Because Volmer, Tafel and Nernst law are based on molarity, the concentration of iron in rich amines must be expressed in mol/L, so, the next table and example shown the way to convert. Iron content in ppm needs to convert to mole/L, $\frac{mole}{L} = \frac{ppm}{55.845*1000}$ all the data after converting as showing from the below Table 4.7:

Table 4.7. Converting iron content in ppm to mole/L

Iron content/ppm	Iron content mol/L	Iron content/ppm	Iron content mol/L
1.62	2.9009E-05	1.23	2.2025E-05
0.77	1.3788E-05	0.59	1.0565E-05
1.37	2.4532E-05	2.71	4.8527E-05
0.73	1.3072E-05	0.93	1.6653E-05
0	1.3072E-05	0.77	1.3788E-05
0.93	1.6653E-05	0.91	1.6295E-05
0.93	1.6653E-05	0.91	1.6295E-05
0	0	1.01	1.8086E-05
1.87	3.3486E-05	0.94	1.6832E-05
0.73	1.3072E-05	1.54	2.7576E-05
0	0	1.21	2.1667E-05
1.09	1.9518E-05	1.08	1.9339E-05
2.71	4.8527E-05	0.77	1.3788E-05
3.11	5.569E-05	0.97	1.737E-05
3.03	5.4257E-05	0.91	1.6295E-05
2.11	3.7783E-05	1.06	1.8981E-05
1.54	2.7576E-05		

4.3.2. Application of Current Density

Determination of current density (i corr), by Bulmer equation: $i = i_0 \left[\exp\left(\frac{\alpha_a zF\eta}{RT}\right) - \exp\left(-\left(\frac{\alpha_c zF\eta}{RT}\right)\right)\right]$. The current density of iron can be determined by i_0 Fe=2FKe [Fe]. exp[$\frac{-\alpha F(Ecorr - E\ Fe)}{RT}$]. And Tafel electro kinetic constant can be determined by: Ke=$10^{((A/T)-B)}$, where, A and B coming from Tafel equation. A= (0.059/ αn) ln j_0; B= (0.059/ αn) = 2.303RT/αF; where, A and B are system specific constants which are fitted from the experimental data. And the equilibrium constant by Nernst law; $E = E^0 + \frac{RT}{NF} ln \frac{[OH]}{[Red]}$, the equation, $mpy = \frac{Kai}{nD}$, is used for calculation of corrosion rates in mpy (mils per year) when the current density calculated. Where, i =current density (A/m^2); i_0 =current density (A/m^2); Z= number of electrons involved in the electrode reaction, F= Faraday constant; R=Universal gas constant, $\alpha_{c=}$ cathodic charge transfer coefficient, dimensionless; α_a = anodic charge transfer coefficient, dimensionless, η= activation over potential, defined as $\eta = (E - E_{eq})$; E=electrical potential V; E_{eq}=equilibrium potential V; a=atomic weight; J=current density; N=number of electron lost; D=density of metallic=3, 2 K, Ke=electro kinetic constant.

Applying this mathematical algorithm over the data shown in 4.3.1 IFe^{+2} can be calculated for each period of time. After those calculations for all the data, the result is shown from Table 4.8.

Table 4.8. Calculation of Icorr and corrosion rate

Fe^{+2} mol/L	**iFe^{+2}**	**V(mpy)**	**Fe^{+2} mol/L**	**iFe^{+2}**	**V(mpy)**
2.90089E-05	4.13462E-13	18.89	1.0565E-05	1.5058E-13	6.88
1.37882E-05	1.96522E-13	8.98	4.85272E-05	6.9166E-13	31.59
2.45322E-05	3.49656E-13	15.97	1.66532E-05	2.3736E-13	10.84
1.30719E-05	1.86313E-13	8.51	1.37882E-05	1.9652E-13	8.98
1.30719E-05	1.86313E-13	8.51	1.62951E-05	2.3225E-13	10.61
1.66532E-05	2.37358E-13	10.84	1.62951E-05	2.3225E-13	10.61
1.66532E-05	2.37358E-13	10.84	1.80858E-05	2.5778E-13	11.77
3.34855E-05	4.77268E-13	21.80	1.68323E-05	2.3991E-13	10.96
1.30719E-05	1.86313E-13	8.51	2.75763E-05	3.9304E-13	17.95
1.95183E-05	2.78194E-13	12.71	2.16671E-05	3.0882E-13	14.11
4.85272E-05	6.91656E-13	31.59	1.93392E-05	2.7564E-13	12.59
5.56899E-05	7.93745E-13	36.26	1.37882E-05	1.9652E-13	8.98
5.42573E-05	7.73327E-13	35.32	1.73695E-05	2.4757E-13	11.31
3.77831E-05	5.38522E-13	24.60	1.62951E-05	2.3225E-13	10.61
2.75763E-05	3.93044E-13	17.95	1.89811E-05	2.7054E-13	12.36
2.20252E-05	3.13925E-13	14.34			

In the range of data from this study the average of corrosion rate is equal to 15.347 mpy Table 4.9 shown time vs iron concentration and corrosion rate. The relation between iron content and corrosion rate can be seen from the Figure 4.3. By making a graph, directly proportional relation between iron content with corrosion rate can be seen as show from Table 4.9 and Figure 4.3.

Table 4.9. Iron content vs corrosion rate

Date	Fe^{+2}/ppm	V(mpy)	Date	Fe^{+2}/ppm	V(mpy)
1-July	1.62	18.89	31-July	1.23	31.59
2-July	0.77	8.98	1-August	0.59	10.84
3-July	1.37	15.97	2-August	2.71	8.98
4-July	0.73	8.51	3-August	0.93	10.61
5-July	0.73	8.51	4-August	0.77	10.61
6-July	0.93	10.84	5-August	0.91	11.77
8-July	0.93	10.84	6-August	0.91	10.96
9-July	0.93	21.80	7-August	1.01	17.95
10-July	1.87	8.51	8-August	0.94	14.11
12-July	0.73	12.71	9-August	1.54	12.59
13-July	0.91	31.59	10-August	1.21	8.98
25-July	1.09	36.26	11-August	1.08	11.31
26-July	2.71	35.32	12-August	0.77	10.61
27-July	3.11	24.60	13-August	0.97	12.36
28-July	3.03	17.95	14-August	0.91	10.98
29-July	2.11	14.34	15-August	1.06	15.35
30-July	1.54	6.88			

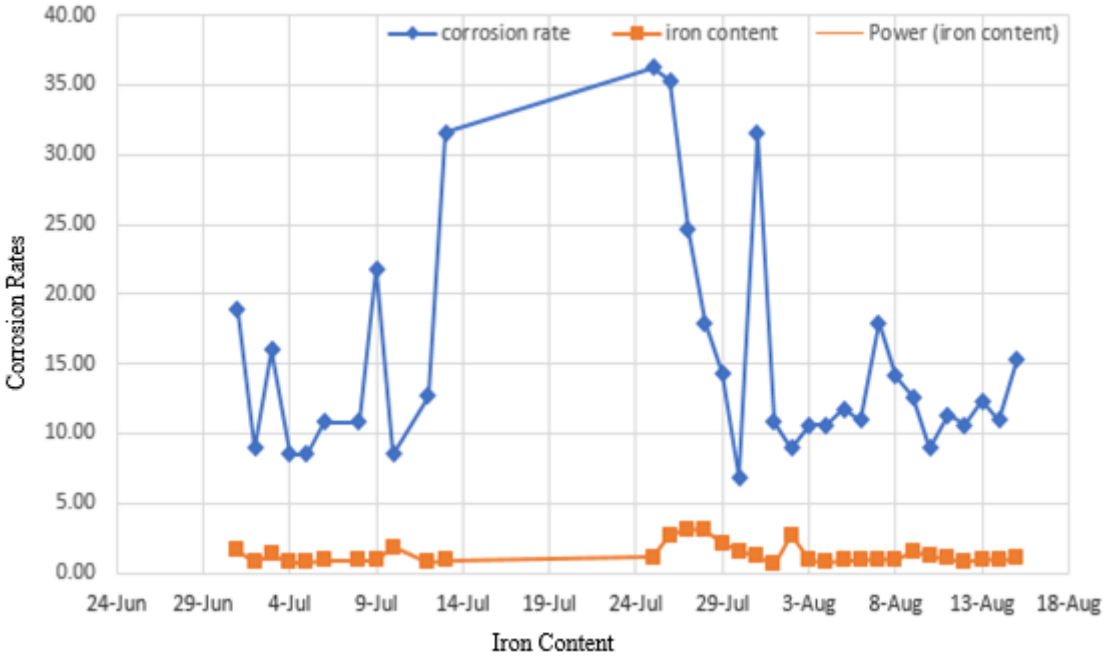

Figure 4.3. The relation between corrosion rates vs. iron content

From the above Figure 4.3 represents the proportional relationship between iron content with corrosion rate, when iron content increased the corrosion rate tends to increase and vice versa.

4.3.3. Relationship between H_2S Loading and Corrosion Rate

Hydrogen sulfide gas makes the MDEA solution corrosive. To study the corrosion behavior of the carbon steel in MDEA solution, the relation of corrosion rate with H_2S loading is necessary as shown from Table 4.10 and Figure 4.4.

Table 4.10. Corrosion rate with H_2S loading of carbon steel in MDEA solution at July/August

Date	H_2S/ppm	V(mpy)	Date	H_2S/ppm	V(mpy)
1-July	39095	18.89	31-July	39136	31.59
2-July	38863	8.98	1-August	39241	10.84
3-July	37511	15.97	2-August	39624	8.98
4-July	38438	8.51	3-August	39868	10.61
5-July	38515	8.51	4-August	52886	10.61
6-July	38901.5	10.84	5-August	37183	11.77
8-July	39288	10.84	6-August	38505	10.96
9-July	37125	21.80	7-August	39827	17.95
10-July	44628	8.51	8-August	39664	14.11
12-July	37386	12.71	9-August	39176	12.59
13-July	37671	31.59	10-August	38322	8.98
25-July	38525	36.26	11-August	39195	11.31
26-July	54513	35.32	12-August	36541	10.61
27-July	55042	24.60	13-August	36613	12.36
28-July	53373	17.95	14-August	33277	10.98
29-July	51915	14.34	15-August	37630	15.35
30-July	43529	6.88			

Using the data from Table 4.10 to make a curve to explain the relation between H_2S loading with corrosion rate can be seen from Figure 4.4.

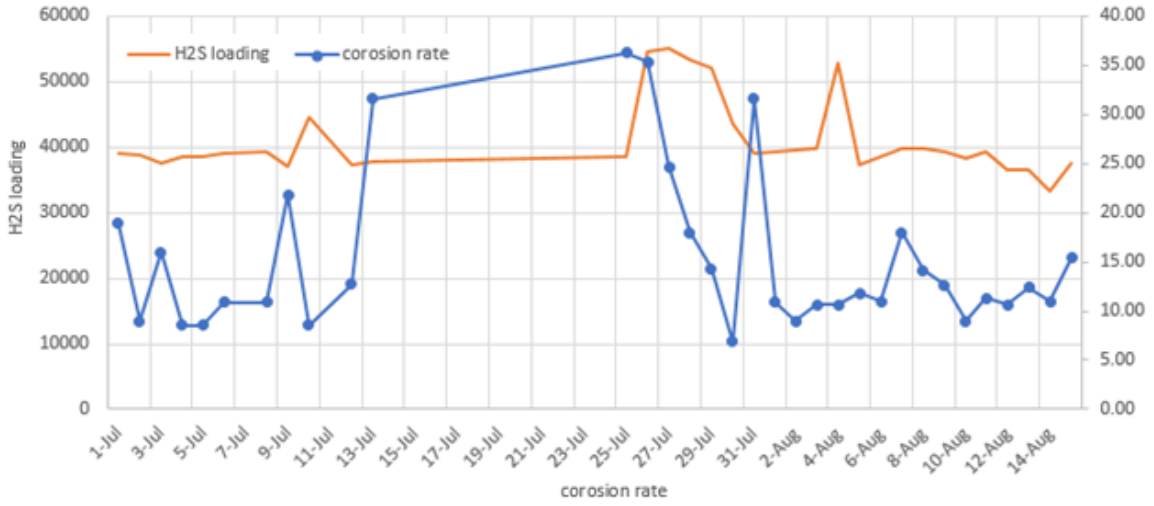

Figure 4.4. The relation between H_2S loading with corrosion rate

Figure 4.4 represents the direct proportional relationship between H_2S loading with corrosion rate according to increasing and decreasing the value of H_2S loading.

4.3.4. Relationship between MDEA Concentration and Corrosion Rate

Khurmala GTP works with 50% solution of MDEA to absorb sour gas, so corrosion rate relationship of carbon steel with methyldiethanolamine (MDEA/H_2S+CO_2) is also necessary as shown from Table 4.11 and Figure 4.5. Table 4.11 contains the data of corrosion rate with amine concentration. And Figure 4.5 show us the relation between corrosion rates with rich amine concentration.

Table 4.11. The relation of corrosion rate with amine concentration

Corrosion rate	[Rich amine]%	Corrosion rate	[Rich amine]%
18.89	46.9	31.59	49.4
8.98	46.7	10.84	----
15.97	46.1	8.98	49.5
8.51	47.7	10.61	49.2
8.51	47.6	10.61	48.8
10.84	----	11.77	48.5
10.84	47.1	10.96	49.6
21.80	48.2	17.95	49.3
8.51	47.2	14.11	49.4
12.71	47.5	12.59	49.1
31.59	47.5	8.98	49.1
36.26	47.2	11.31	48.6
35.32	47.9	10.61	48.7
24.60	47.8	12.36	48.7
17.95	48.1	10.98	48.9
14.34	48.3	15.35	49.1
6.88	50.1		

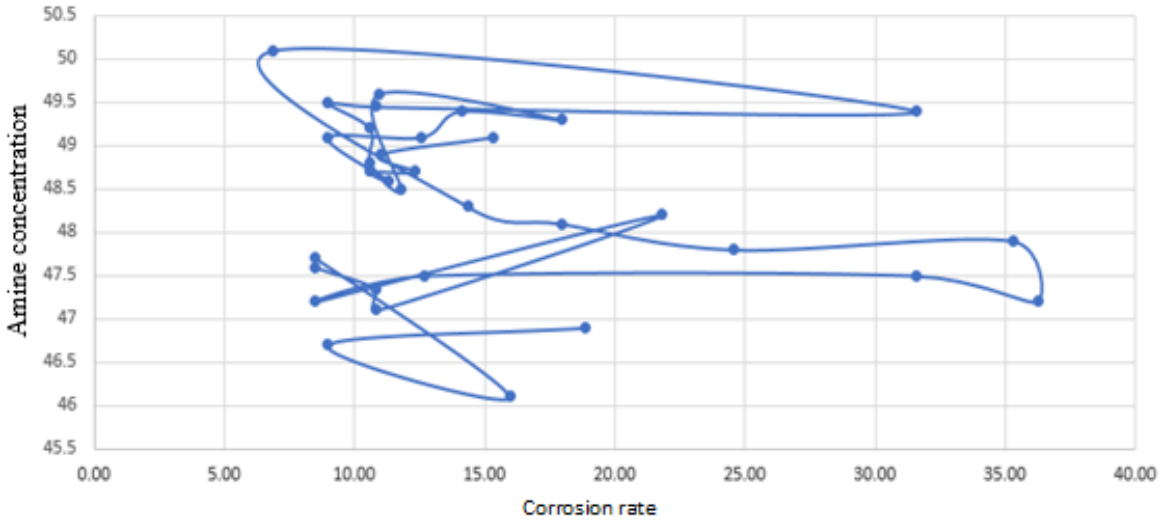

Figure 4.5. The relation between amine concentrations with corrosion rate

From Figure 4.5 can be seen that there is no apparent relationship between amine concentrations with corrosion rate according increasing or decreasing amine concentration. It means amine solutions itself is non-corrosive but the presence of H_2S gas makes that solution corrosive.

4.3.5. The Relationship between H_2S and Iron Content

Corrosion due to H_2S is mainly electrochemical in nature. The products of dissociation of H_2S gas are aggressive and can catalyze the electrochemical reactions, especially the dissolution of Fe to form iron sulfide FeS, therefore the study of H_2S loading with iron content is more important as shown from the next table and graph. Table 4.12 contains the data of iron content with H_2S loading in unit of ppm. The Figure 4.6 explained the relation between iron content with H_2S loading.

Table 4.12. Iron content with H_2S loading

Fe^{+2}/ppm	H_2S/ppm	Fe^{+2}/ppm	H_2S/ppm
1.62	39095	1.23	39136
0.77	38863	0.59	39241
1.37	37511	2.71	39624
0.73	38438	0.93	39868
0.73	38515	0.77	52886
0.93	38902	0.91	37183
0.93	39288	0.91	38505
0.93	37125	1.01	39827
1.87	44628	0.94	39664
0.73	37386	1.54	39176
0.91	37671	1.21	38322
1.09	38525	1.08	39195
2.71	54513	0.77	36541
3.11	55042	0.97	36613
3.03	53373	0.91	33277
2.11	51915	1.06	37630
1.54	43529		

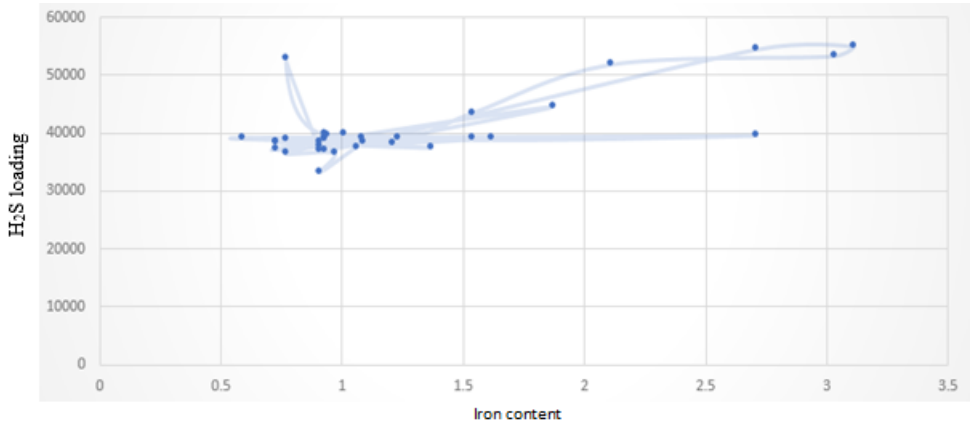

Figure 4.6. The relation of H_2S loading with iron content

From Figure 4.6, it is obvious that with the increase of H_2S concentration the value of iron content is also increased due to formation of more protonated amine ions ($R_2NH_2^+$). The greater the concentration of protonated amine ions, the greater will be the dissolution of iron. So, there is a direct proportional relationship between them.

4.3.6. Overall Corrosion Rate with Icorr

The electrochemical corrosion rate measurements often provide results in terms of electrical current. And the conversion of these current values into mass loss rates or penetration rates is based on Faraday's Law, Table 4.13 and Figure 4.7 showed the relation between $i$corr with corrosion rate.

Table 4.13. Corrosion rate with Icorr

Icorr	**icorr*10^{13}**	**CR**	**Icorr**	**icorr*10^{13}**	**CR**
4.1346E-13	4.13	18.89	6.9166E-13	6.92	31.59
1.9652E-13	1.97	8.98	2.3736E-13	2.37	10.84
3.4966E-13	3.50	15.97	1.9652E-13	1.97	8.98
1.8631E-13	1.86	8.51	2.3225E-13	2.32	10.61
1.8631E-13	1.86	8.51	2.3225E-13	2.32	10.61
2.3736E-13	2.37	10.84	2.5778E-13	2.58	11.77
2.3736E-13	2.37	10.84	2.3991E-13	2.40	10.96
4.7727E-13	4.77	21.80	3.9304E-13	3.93	17.95
1.8631E-13	1.86	8.51	3.0882E-13	3.09	14.11
2.7819E-13	2.78	12.71	2.7564E-13	2.76	12.59
6.9166E-13	6.92	31.59	1.9652E-13	1.97	8.98
7.9375E-13	7.94	36.26	2.4757E-13	2.48	11.31
7.7333E-13	7.73	35.32	2.3225E-13	2.32	10.61
5.3852E-13	5.39	24.60	2.7054E-13	2.71	12.36
3.9304E-13	3.93	17.95	2.5778E-13	2.58	10.98
3.1392E-13	3.14	14.34	3.33E-13	3.33	15.35
1.5058E-13	1.51	6.88			

Figure 4.7 is related to the relation of corrosion rate with Icorr. From Figure 4.7 can be seen that corrosion rate increased with increasing of $i$corr, and there is a very strong

directly proportional relationship between them when $i$corr increased and corrosion rate increased directly, according the Equation 2.16.

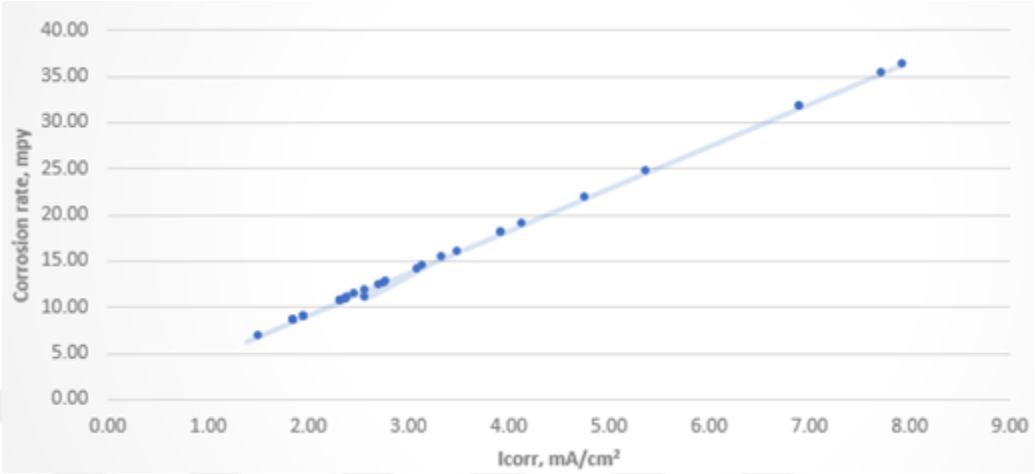

Figure 4.7. The relation of corrosion rate with Icorr

4.4. Evaluation of Results by Comparison of Corrosion Rate with International Standards Specifications

Averaged corrosion rates for carbon steel				
Velocity [ft/s]	H2S loading as molar ratio to MEA			
	0.2	0.4	0.6	0.8
0	0	0	1	1
20	8	12	12	12
40	12	14	16	20
60	13	16	20	43
80	16	18	25	66

Six levels are:

	< 5 mpy
	5 - 10 mpy
	10 - 15 mpy
	15 - 20 mpy
	20 - 50 mpy
	> 50 mpy

Negligible corrosion.
Good/ on control.
Allowance/ on control.
High/ over control
Important / out control.
Severe / extreme

Figure 4.8. Corrosion rate classification according to permasense

After determining the corrosion rate in GTP by iron content and Volmer–Tafel laws relationships is necessary to determine how this corrosion rate can be considered into industrial standards in order to define actual conditions and if is also necessary to make improvements into sweetening process to maintain the production process in quality control of corrosion process. According to Permasense (2016), the corrosion process can be classified in 6 levels depending on the corrosion rate (mpy) and sour gas velocity into contactor (V_{gas}) those levels are shown in Figure 4.8.

At GTP at typical daily flow production of 45 MMSCF/D the V_{gas} is 27.08 ft/s and H_2S loading is 0.41, the actual corrosion rate is 15.35 mpy so, comparing this results using Permasense criteria, GTP corrosion rate can be classified as High/over control, that's means, corrosion process is occurring but in a level that is sensible at changing production conditions, so if in any way, Vgas is increased or increase H_2S loading in rich amine with same Vgas, this condition will displace from level 4 to level 5, that's from high/over control to: important/out of control of corrosion rate (Actual rate: 15.35 mpy > 13 mpy maximum at V_{gas}=27.08 ft/s and mol H_2S/mol MDEA: 0.41), details about this calculation can be observed at Figure 4.9.

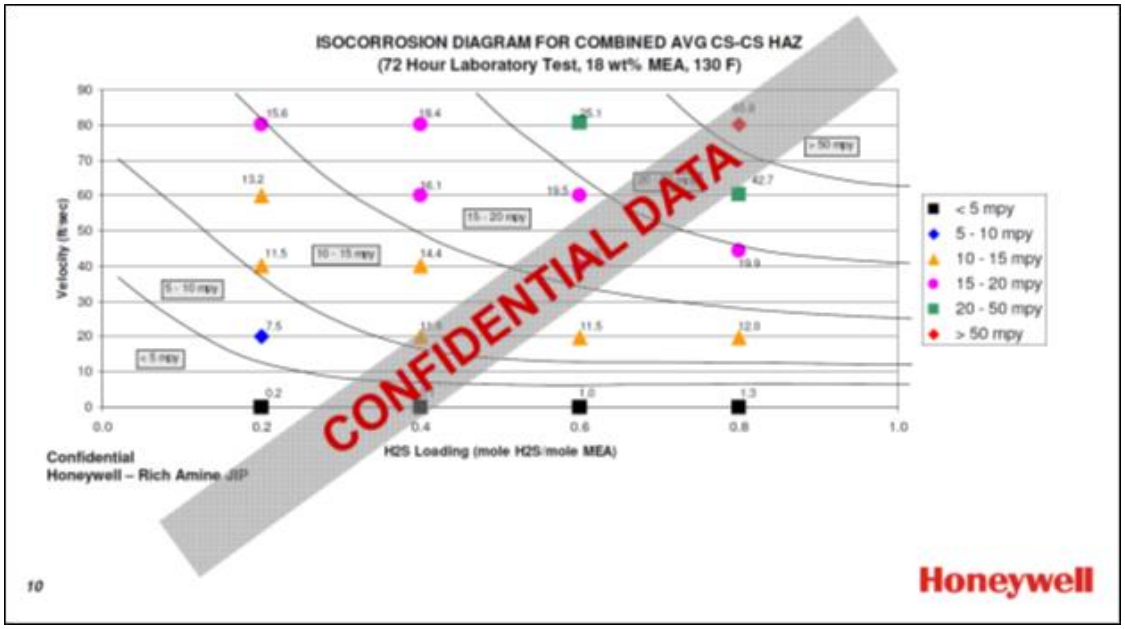

Figure 4.9. Corrosion rate classification according to Honeywell

Because V_{gas} is international table and monograms is the reference is necessary with process data calculate is based on normal condition and data: F=45 MMSCFD; diameter = 7 ft; r= 3.5 ft: converting sour gas flow MMSCFD to SCft; base: 1 hour of flow; $\mathrm{F} = 45\ \mathrm{MMSCFD} * \frac{1000{,}000\mathrm{SCF}}{1\mathrm{MM}} * \frac{1D}{24h}$; F=1,875,000 SCft; $A = \pi r^2 = 3{,}14\ \left(\frac{7}{2}\right)^2 = 38{,}465\ \mathrm{ft}^2$; $V = \frac{F}{A} = \frac{1{,}875000}{38{,}465} = 4874561\ ft/h$; $\mathrm{V} = \frac{48745{,}61\mathrm{ft}}{\mathrm{h}} * \frac{1\mathrm{h}}{36005} = \frac{13{,}54\mathrm{ft}}{\mathrm{s}}$; V=13,554 ft for one train, because there is two trains: V=13,554 * 2 and V=27.08. This condition can be get worse if is achieved one of these processing scenarios: increased H_2S loading over 0, 4 at same V_{gas}, increased V_{gas} at actual stable H_2S loading, increasing both V_{gas} and H_2S loading. Those scenarios can be achieved for example, if production is increased over 43 MMSCF/D with sour gas inlet with H_2S and CO_2 acid gas loading over around 10% mol. In order to ensure comparison and evaluation results another impartial and relevant reference was used, in this case, the Specialized Bench marketing Company Honeywell have develop a software that can estimate corrosion rate in amine sweetening complex using Volmer-Tafel laws and on field data over than more 30 different amine units around the word, this software named Predict-Amine 2.0 is capable of determining in automatized real-time approach the corrosion rate of any sweetening process based on amine chemistry. Due to the fact this software has a specific license patent have confidential data couldn't be obtained, but for the purpose of this study extrapolation behavior of some generalized charts was used, this because, at over polarized current conditions it well understood MDEA and MEA have equivalent electrochemical corrosion mechanism. Figure 4.9 can be seen the Predict-Amine 2.0 shown relationship V_{gas}, H_2S loading and catalogued corrosion levels.

In that monograph can be observed the operational point of (15.35 mpy; 0.41 H_2S loading) is situated at orange color, means at level of 10 – 15 mpy**,** so is classified as high corrosion but on control level, similar classification of Permasense cataloguing happened, by this way also can be concluded the corrosion process at GTP unit in running border line between at important corrosion rate because of high loading charge and maximum velocity achieved at amine contactor.

It is important to mention, that this value is an overall corrosion rate is not a specific value over any part of the system instead must be considered as generalized value so, in

some sensitive areas like: contactor bottom (V201, V101), top and condensers of Still Columns, and Flash drums are not determined specifically because of lack of data.

The evaluation results can be summarized as Table 4.14 shown. Interpreting these results correctly attached to this international references GTP. Corrosion rate is situated in high corrosion rate level in some place between 3 and 4 international corrosion classifications.

Table 4.14. Summarized evaluation results

Evaluation parameter	**Permasense criteria**	**Honeywell Criteria**
Actual corrosion rate	Max 13 mpy 15.35 mpy	Range: (10 – 15) mpy 15.35 mpy
Classification rate	High/ on control	High/on control
Level	4	3

5. CONCLUSIONS

After obtained results and evaluation some important statements may be declare:

- Iron determination by molecular absorption spectroscopy is a highly reproducible, trustworthy, readable, precise and accuracy analytical method for MDEA applications; as analytical quality control have accuracy of 97.05% and precision of 99.92% with a standard deviation of 0.08% and analytical error less than 3%.

- Corrosion rate estimation based on Volmer–Tafel–Nernst laws are convenient for determining corrosion classification level for sweetening amine gas treatment chemical plants, when the mainly corrosion mechanism is electrochemical type.

- Corrosion process in GTP is mainly occurring at overpotential level.

- Corrosion rate of 15.35 mpy gives an intermediate corrosion classification of 4, that's mean, corrosion on GTP is high but still on control, any factor associated to increase velocity, H_2S loading, or composition of sour gas inlet will move this point to a worse condition (level 5: important or 6: severe corrosion).

- Chemical interferences analyzing Fe in MDEA solvent need accurate and delicate techniques, any deviation from this procedure will get wrong results.

- Corrosion rate releasing iron to MDEA solvent stream is mainly dependable of: a) flows of gas and lean amine, b) acid gas loading at sour gas inlet, c) H_2S loading in solvent all of this, in absence of oxygen.

- Update of corrosion rate should be made twice a year or, when typical process conditions are increased and working for a stable period.

- Would be necessary to decide the time, dosage, concentration and type of corrosion inhibitor to apply when working conditions at GTP change from level 4 to level 5.

- Automatize this calculation to be easier next time when corrosion rate estimation will be run again.

REFERENCES

Abollino O, Aceto M, Acchero S, Saarzanni C, Mentasti E (1995) Determination of copper, cadmium, iron, manganese, nickel and zinc in antarctic sea-water - comparison of electrochemical and spectroscopic procedures. Analytica Chim Acta 305: 200-206

Abdulrahman R, Kamal I, Ali J (2015) Natural gas desulfurization process by mea amine: the preferable engineering design procedure. International journal of engineering trends and technology. Iraq

Addington F, Hendrix D (2000) Aggressive corrosion of 316 stainless steel in amine unit: causes and cures. Huston Texas Paper No. 00698. USA

Akpa Jackson G (2013) Modeling of the corrosion rate of the stainless steel in marin oil environment. ISSN 1819-6608. Rivers State, Nigeria

American Standards of Testing and Materials (1997) Standard Practice for Preparation, Standardization and Storage of Standard and Reagents for Chemical Analysis. E200

American Standards of Testing and Materials (1999) Standard Practice for Calculation of Corrosion Rates and Related Information from Electrochemical measurements. G 102

American Standards of Testing and Materials (2003) Standard Test Method for Analysis of Natural Gas by Gas Chromatography. D1945

Aranaz I, Mengíbar M, Harris R, Paños I, Miralles B, Acosta N, Heras, Á (2009) Functional characterization of chitin and chitosan. Current Chemical Biology 3(2): 203-230

Arthur LC, Scott WW, Dennis KN (2005) MPR Services Inc., Dickinson Texas (2005). Corrosion and Corrosion Enhancers in Amine System. Canada: Banff, Alberta

Bagotsky S. (2006). Fundamentals Of Electrochemistry. Moscow, Russia

Basheer K, Adebayo1, Según Ayejuyo1, Hussein K, Okoro B, Ximba J (2011) Spectrophotometric Determination of Iron In Tap Water Using 8-Hydoxyquinoline as a Chromogenic Reagent. African Journal of Biotechnology 1: 16051-16057

Behera S, Ghanty S, Ahmad F, Santra S, Banerjee S (2012) UV-Visible Spectrophotometric Method Development and Validation of Assay of Paracetamol Tablet Formulation. West bangal, India: 2155-9872

Blanty P, Kvansuiclka F, Kendler E (1997) Trace determination of iron in water at the µg/l level by on-line coupling isotachophoresis and capillary zone electrophoresis with UV detection of EDTA-Fe (III) complex. J Chrom A 757:2979-2302

De Broglie M (1913) Sur une nouveau procédé permettant d'obtenir la photographie des spectres de raies des rayons Röntgen. Comptes Rendus 157: 924-926

De Hoffmann E, Stroobant V (2007) Mass spectrometry: principles and applications. John Wiley & Sons

Douglas H, Mackenzie Christina A, Daniels Jerry A (1987) Design & Operation of a Selective Sweetening Plant Using MDEA.USA, pp 31-36

Dupart M, Bacon T, Edwards D (1993) Understanding Of Corrosion In Alkanolamine Gas Treating Plant. Texas, USA, pp 89-94

Einar B (2004) Corrosion and Protection. Trondheim, Norway ISBN 13: 978-1-85233-758-2

El-Feki A (1999) Mathematical Modeling of Corrosion Measurement. Doctor of philosophy University of Wollongong

Farshad FF, Garber J, Rieke Komaravelly S (2010). Predicting Corrosion in Pipelines, Oil Wells and Gas Wells; a Computer Modeling Approach. Iran, pp 86-96

Gandhimathi R, Vijayaraj S, Jyothirmaie M (2012) Analytical Process of Drugs by Ultraviolet (UV) Spectroscopy-A review. Andhra Pradesh, India, pp 72-78

Gotsche N, Ulbricht H, Arndt M (2007) UV-VIS Spectroscopy of Large Molecules for Applications in Matter Interferometry. Austria, pp 583-589

Gray J, Sahajwalla V, Paramagrur R (2005) Kinetics and Mechanism of Corrosion of Laboratory Hot briquetted iron. 36B: 614-615

Hajilary N, Ehsani A, Sheikhae N, Foroughipour H (2011) Amine Gas Sweetening Problems Arising From Amine Replacement and Solutions to Improve System Performance. Assaluyeh, Iran, pp 24-30

Hardesty J, Attili B (2010) Spectrophotometry and the Beer-Lambert Law: An Important Analytical Technique in Chemistry. Colling College. USA

Hunger M, Weitkamp J (2001) In situ IR, NMR, EPR, and UV/Vis spectroscopy: Tools for new insight into the mechanisms of heterogeneous catalysis. Angewandte Chemie International Edition 40(16): 2954-2971

Huntsman Standard Method (2001) Method of Test for the Alkalinity of Soluble Water Closest Amine.st 5: 5-01

Ieaghg (2010) Corrosion and Materials Selection In Ccs System. UK

International Standardization Organization (1999) General Requirements for the Competence of Testing and Calibration Laboratories. IEC19025

Jamaluddin A, Nazrul I (2015) The Most Dangerous Job on the Planet Ship Braking In Bangladesh. Bangladesh. Asia

Kasaai MR (2010) Determination of the degree of N-acetylation for chitin and chitosan by various NMR spectroscopy techniques: A review. Carbohydrate Polymers 79(4): 801-810

Kulkarni S (2015) A Review on Studies and Research on Corrosion and Its Prevention. India, P-ISSN: 2454-2237

Kumirska J, Czerwicka M, Kaczyński Z, Bychowska A, Brzozowski K, Thöming J, Stepnowski P (2010) Application of spectroscopic methods for structural analysis of chitin and chitosan. Marine Drugs 8(5): 1567-1636

Lancaster KM, Finkelstein KD, DeBeer S (2011) Kβ X-ray Emission Spectroscopy Offers Unique Chemical Bonding Insights: Revisiting the Electronic Structure of Ferrocene. Inorganic Chemistry 50(14): 6767-6774

Laquai K, Melhuish W, Zander M (1988) Molecular Absorption Spectroscopy Ultraviolet and Visible (UV/VIS), Great Britain, pp 1449-1460

Mackenzie D, Daniels C, Bullin J (2006) Design & Operation of a Selective Sweetening Plant Using MDEA. Bryan, Texas. USA

Mark of Schlumbergr (2016) Amine Gas Sweetening System. 16-PRS-180203

Monica F, Macocian E, Toderas M, Caraban A (2012) Spectrophotometric Measurement Techniques for Fermentation Process, part one base theory for UV-VIS Spectrophotometric determination. Hungary–Romania

National Association of Corrosion Engineers (NACE International) (1999) Techniques for Monitoring Corrosion and Related Parameters in Field Applications. Canada, Publication 3T199, Item No. 24203

Navabzadeh S, Brown B, Nesic S (2016) Verification Of Electrochemical Model for Aqueous Corrosion of Mild Steel for H_2S Partial Pressure Up To 0.1 mPa. Ohio University, pp 144-154

Nielsen R, Lewis K, McCullough J, Hansen D Controlling Of Corrosion in Amine Treating Plants. Sugarland USA

Oyelami B, Oyediran A, Abraham A, Mathematical modeling: An application to corrosion to petroleum industry. National Mathematical Centre Abuja, Nigeria

Pavel B, Frantisek K, Erust K (1997) Trace Determination of Iron in Water at the μg/l Level by Online Coupling Isotachophoresis and Capillary Zone Electrophoresis with UV Detection of the EDTA-Fe (III) Complex. J. Chrom. A. 757: 2979-2302

Peter A, De Paula J (2006) Physical Chemistry for the Life Sciences, Oxford.UK

Rennie S (2006) *Corrosion and Material Selection for Amine Service*. Australia

Robergs R (2010) FASEP, EPC. Spectrophotometry

Roy U, Ahmed M (2009). A Simple Spectrophotometric Method for the Determination of Iron (II) Aqueous Solutions. Chittagong-Bangladesh, 709 – 726

Samina M, Karim A, Venkatachalam A (2011) Corrosion Study of Iron and Copper Metals and Brass Alloy in Different Medium. India, S344-348

Sharma BK (2007) India *Spectroscopy,* Received form http://google.books.com

Skoog D, West M, Holler F, Crouch S (2005). Analytical Chemistry: An Introduction, 7th ed., Chapters 21 and 22, pp 547-592

Srinivasan S, Lagad V Prediction of Amine Corrosion in Refinery and Gas Processing Rich Amine Circuits. Honeywell

Standards and Research Department (1997).Engineering Standard for Process Design of Gas Treating Units Part1- Process Design of Gas Sweetening Units. Karimkhan Avenue, Tehran, Iran, IPS-E-PR-551

Suleiman I, Oloche O, Yaro S (2013) The development of a mathematical model for the prediction of corrosion rate behaviour for mild steel in 0.5 M sulphuric acid. Nigeria, 9

Sun W, Nesic S, Papavinasam S (1998) Kinetic Of Iron Sulfide and Mixed Iron Sulfide/Carbonate Scale Precipitation in CO_2/H_2S Corrosion. Canada, paper 06644

Turner M (2012) Finite Element Modeling of Galvanic Corrosion of Metals. Master of Engineering in Mechanical Engineer, Rensselaer Polytechnic Institute Hartford, CT

Universal Oil Processing (1981) Apparent Hydrogen Sulfide in Amine Solutions. Method 827

Wei S, Srdjan N (2006) Kinetics of iron sulfide and mixed iron sulfide/carbonate scale precipitation in CO_2/H_2S corrosion. USA

West C (2008) Efficient use of fuel gas in Amine. Module 14 of 17

Wineland D, Wayne M, Itano, Bergquist JQ (1987) Absorption spectroscopy at the limit: detection of a single atom. Boulder, Colorado 389

Wong L, Martin S, Rebak B (2006) Methods to Calculate Corrosion Rates For Alloy 22 from Polarization Resistance Experiments. British Columbia, Canada, PVP2006-ICPVT11-93421

Zare H, Mirzaei S (2009) Removal of CO_2 and H_2S Using Aqueous Alkanolamine Solutions. World Academy of Science, Engineering and Technology, Vol: 3, No: 1

CURRICULUM VITAE

Pirdawood Hogr

Laboratory Supervisor

KAR oil and Gas GROUP

Makhmour District, Erbil, Iraq

Email:hogromar90@yahoo.com

Phone: +964 750 7323490

Hogr has been working in Gas Treatment Plant for 4 years. He is a Laboratory Supervisor for the Sweetening and Drying Gas Complex based in Amine Treatment Process at KAR GROUP, Kurdish region, Iraq. This Laboratory is responsible for supporting Gas Quality Control and sub products Streams MDEA and Tri ethylene Glycol also has a Chemist Role as Technical Support including performance, products quality certification for downstream 600MW Khormala Power Plant. Hogr also provides a range of training both internally within Laboratory Analysts as well as to external groups. Hogr was awarded as author of research: "Hogr O. Pirdawood (2017). Determination of relationship between pH and acid loading in gas treatment plant (amine unit), 2nd European Organic Chemistry Congress, Volume 6, issue 1, ISSN: 2161-0401." for Organic Chemistry Conferences at Amsterdam, the Nederland. Has a degree as Chemist from the University of Salahaddin and undergraduate Master degree in Analytical Chemistry at the Bingöl University.